# Improved Spectral Coverage and Fluorescence Quenching in Donor-acceptor Systems Involving Indolo[3-2-b]carbazole and Boron-dipyrromethene or Diketopyrrolo-pyrrole†

Adis Khetubol[1], Sven Van Snick[2], Melissa. L. Clark[2], Eduard Fron[1], Eduardo Coutiño-González[1], Arvid Cloet[1], Koen Kennes[1], Yuliar Firdaus[1], Maarten Vlasselaer[2], Volker Leen[2], Wim Dehaen[2], Mark Van der Auweraer[1*]

[1]. Molecular Imaging and Photonics, Chemistry Department, KULeuven, Celestijnenlaan 200F, B2404, 3001, Leuven, Belgium, [2]. Molecular Design and Synthesis, Chemistry Department, KULeuven, Celestijnenlaan 200F, B2404, 3001, Leuven, Belgium

*Corresponding author e-mail: Mark.Vanderauweraer@chem.kuleuven.be (Mark Van der Auweraer)

† This manuscript is part of the Special Issue dedicated to the memory of Michael Kasha

## ABSTRACT

A novel π-conjugated triad and a polymer incorporating indolo[3,2-*b*]-carbazole (ICZ) and 4,4-difluoro-4-bora-3a,4a-diaza-s-indacene (BODIPY) were synthesized via a Sonogashira coupling. Compared to the parent BODIPY the absorption and fluorescence spectrum were for both compounds broader and red-shifted. The red-shift of the fluorescence and the decrease of the fluorescence quantum yield and decay time upon increasing solvent polarity were attributed to the formation of a partial charge transfer state. Upon excitation in the ICZ absorption band the ICZ fluorescence was quenched in both compounds mainly due to energy transfer to the BODIPY moiety. In a similar ICZ-π-DPP polymer, (where DPP is diketopyrolopyrrole), a smaller red shift of the absorption and fluorescence spectra compared to the parent DPP was observed. A less efficient quenching of the ICZ fluorescence in the ICZ-π-DPP polymer could be related to the unfavorable orientation of the transition dipoles of ICZ and DPP. The rate constant for energy transfer was for all compounds an order of magnitude smaller than predicted by Förster theory. While in a solid film of the triad a further red-shift of the absorption maximum of nearly 100 nm was observed, no such shift was observed for the ICZ-π-BODIPY polymer.

## INTRODUCTION

In the search for alternative energy sources organic material based photovoltaics (OPVs) have been successfully explored as a viable alternative to Si-based solar cells for some applications (1,2,3). The driving force for this attention devoted to OPVs, based on both small molecules and polymers, is largely determined by their advantageous properties such as, low weight, easy processability, high absorption coefficients.

The obvious advantages notwithstanding, to date, OPVs suffer from a suboptimal power conversion efficiency and operational lifetime, limiting their large scale introduction to the market. To improve the device efficiencies, several strategies have been proposed and investigated with varying success (4,5,6,7,8,9). One such strategy is to improve the photocurrent generated by the device which depends among other factors on the efficiency of light absorption, and exciton dissociation (3,4). To increase the efficiency for light absorption, a better coverage of the terrestrial solar emission spectrum is necessary (10,11,12,13,14,15). This can be achieved in donor-acceptor (D-A) combinations where the absorption spectrum is shifted to longer wavelengths corresponding to a smaller optical band gap (16,17,18,19,20,21). Furthermore, using such conjugated D-A combinations where the HOMO and LUMO are confined to different parts of the chromophore, can increase the efficiency of exciton dissociation and decrease that of geminate electron hole recombination (16,17,18,19,20). In D-A polymers the donor and acceptor are often connected by an olefinic or acetylenic linker acting as a charge mediator, however, acetylenic spacers have been shown to yield higher power conversion efficiencies for bulk heterojunctions (22,23,24).

Indolo[3,2-*b*]-carbazoles (ICZs) with different substitution patterns and polymers thereof have been investigated for use in organic electronic applications such as organic field effect transistors (OFETs) (25,26,27,28,29), organic light emitting diodes (OLEDs) (30,31,32,33), organic photovoltaics (OPVs) (34,35,36), and dye sensitized solar cells (DSSCs) (37). We recently reported a short and high yielding alternative route towards 2,8-difunctionalized indolo[3,2-*b*]carbazole which has demonstrated to be a versatile building block (38). Due to its relatively large optical band gap, large molar extinction coefficient, relatively long singlet decay time and a moderate fluorescence quantum yield (39), ICZ can be considered as a suitable donor in a system involved electron or energy transfer, when linked to an appropriate acceptor building block.

We employed in this work 4,4-difluoro-4-bora-3a,4a-diaza-s-indacene (BODIPY) as the acceptor due to its excellent properties such as high molar extinction coefficient, excellent thermal and photochemical stability, and good solubility (40). Moreover, our building block synthesis allows us to develop many different BODIPY analogues with emission wavelengths tunable from 500 to over 700 nm, by attaching supplementary units at different positions (41,42,43,44,45,46,47).

As a comparison, diketopyrrolo pyrrole (DPP) is also employed as the acceptor moiety. DPP has been demonstrated to be a good co-monomer for thiophene based D-A conjugates and polymers as it allows for the synthesis of small molecules and copolymers combining a broad absorption, in the visible with a small optical band gap and, high thermal stability and charge carrier mobility (48,49,50,51,52). We hereby report on the synthesis and spectroscopic properties of small molecule and polymeric D-A materials using indolo[3,2-*b*]-carbazole (ICZ)

and 4,4-difluoro-4-bora-3a,4a-diaza-s-indacene (BODIPY) or diketopyrrolo-pyrrole (DPP), to be used as an efficient light harvesting system both in solution and in films.

## MATERIALS AND METHODS

**Materials:** All solvents, used for spectroscopic studies are of spectroscopic grade and were purchased from Sigma-Aldrich and Acros. They were used without a further purification. The compounds ICZ 1 (38), BODIPY 1 (53), BODIPY 2 (53), and DPP 2 (54) were prepared according to literature methods.

***Synthesis of the ICZ-π-BODIPY triad (triad 1),*** a round-bottomed flask was loaded with BODIPY 1 (150 mg, 0.42 mmol), ICZ 1 (181.5 mg, 0.29 mmol), CuI (2 mg, 2.5 mol%), $Pd(PPh_3)_4$ (2 mg, 1 mol%) and flushed with Ar, THF (1 mL) and *i*$Pr_2NEt$ (5 mL) were then added (Scheme 1). This mixture was heated to reflux for one hour and then allowed to cool to room temperature. The reaction mixture was dissolved in DCM and run through a celite pad. The organic layer was concentrated and the resulting solid was purified by silica gel chromatography ($CH_2Cl_2$:petroleum ether 1:1) to yield pure product of triad 1 as a dark purple powder (24% yield). mp: >300°C; $\delta_H$ (300 MHz; $CDCl_3$) 0.88 (10 H, m), 1.05-1.25 (8 H, m), 1.47 (4 H, m), 2.45 (6 H, s), 2.58 (6 H, s), 2.60 (6 H, s), 3.78 (4 H, t, J 8.1), 6.21 (2 H, s), 6.62 (2 H, s), 7.13 (2 H, s), 7.21 (2 H, d, J 4.05), 7.47 (2 H, d, J 9.78), 7.66 (10 H, m); No adequate $^{13}C$ spectrum could be obtained for the triad using the 75 MHz or the 100 MHz probe.

**Scheme 1**

***Synthesis of the ICZ–π–BODIPY polymer (polymer 1),*** a round-bottomed flask was loaded with BODIPY 2 (50 mg, 0.1 mmol), ICZ 1 (62.4 mg, 0.1 mmol), CuI (1 mg, 2.5 mol%), $Pd(PPh_3)_4$ (1 mg, 1 mol%) and flushed with Ar, THF (2 mL) and *i*$Pr_2NEt$ (1 mL) were then added (Scheme 2). The reaction mixture was heated to reflux and allowed to stir overnight. The resulting dark-blue solution was concentrated under reduced pressure, providing a dark-blue powder which was purified by Soxhlet extraction, firstly with $CH_3OH$, then acetone, then hexane and finally THF. A black powder with $M_n$ of 4.4 kg/mol and PDI of 2.5 was obtained when the THF fraction was concentrated under reduced pressure. Yield: 46%. $\delta_H$ (300 MHz; $CDCl_3$) 0.80-1.35 (20 H, bs), 2.20 (9 H, bs), 2.59-2.74 (6 H, bs), 3.76 (4 H, bs), 6.51 (2 H, bs), 6.92 (4 H, bs), 7.16 (4 H, bs), 7.61 (10 H, bs).

**Scheme 2**

***Synthesis of the ICZ–π–DPP polymer (polymer 2),*** a round-bottomed flask was charged with ICZ 1 (100 mg, 0.16 mmol), DPP1 (98 mg, 0.16 mmol), CuI (1.2 mg, 0.006 mmol), $Pd(PPh_3)_2Cl_2$ (2.3 mg, 0.003 mmol) and flushed with Ar, THF (5 mL) and *i*$Pr_2NH$ (5 mL) were then added (Scheme 3), the reaction mixture was heated to reflux and stirred overnight. The resulting dark-red solution was concentrated under reduced pressure, providing a dark-red powder which was purified by Soxhlet extraction with $CH_3OH$, acetone, hexane and finally $CHCl_3$. A dark-red powder with $M_n$ of 3.6 kg/mol and PDI of 1.5 was obtained when the $CHCl_3$ fraction was concentrated under reduced pressure. Yield: 46%. $\delta_H$ (300 MHz; $CDCl_3$) 0.87 (10 H, bs), 1.16-1.24 (8 H, bs), 1.55 (4 H, bs), 3.79 (4 H, bs), 6.68 (2 H, bs), 7.25 (4 H, bs), 7.53-7.84 (20 H, bs).

**Scheme 3**

***Synthesis of DPP 1,*** a round-bottomed flask was loaded with DPP 2 (1200 mg, 3.9 mmol), $K_2CO_3$ (2209 mg, 16 mmol) and DMF (25 mL). The reaction set-up was flushed with Ar and heated to 140°C, then hexyl bromide (2.24 mL, 16 mmol) was added in one portion (Scheme 4). The reaction was allowed to stir overnight at 140°C and subsequently poured into ice-water (500 mL). The resulting precipitate was filtered and washed with $CH_3OH$. The compound was obtained in 33% yield as a dark-red solid. Mp: 176.2- 177.3 °C; δH (300 MHz; $CDCl_3$) 0.83 (6 H, t, J 6.2), 1.20-1.23 (12 H, m), 1.51-1.54 (4 H, m), 3.72 (4 H, t, J 7.5), 7.62-7.68 (8 H, m); δC (75 MHz; $CDCl_3$) 13.9, 22.4, 26.3, 29.4, 31.2, 41.8, 109.9, 125.8, 126.9, 130.1, 132.2, 147.4, 162.4. MS(EI): m/z 468([M]+,100%).

**Scheme 4**

**Experimental details,** Steady-state absorption and corrected photoluminescence (PL) spectra were recorded with a Lambda 40 (Perkin-Elmer) spectrophotometer and Horiba Jobin Yvon Fluorolog FL3-22 fluorometer, respectively. The fluorometer allowed us to correct the spectra for the wavelength dependence of the sensitivity of the detection system and of the intensity of the excitation beam.

The fluorescence decays were determined by the single photon timing (SPT) method. The excitation wavelengths of 410 nm and 488 nm were obtained using the second harmonic of a Ti:sapphire laser (Tsunami, Spectra Physics). The Ti:sapphire laser was pumped by an intracavity frequency doubled Millenia laser (Spectra Physics). For the excitation at 550, 635 nm and 644 the output of an OPO (GWU), pumped by the Ti:sapphire laser, was frequency doubled. The detection system consisted of a subtractive double monochromator (9030DS, Sciencetech) and a microchannel plate photomultiplier (R3809U, Hamamatsu). Fluorescence

decays were recorded under magic angle polarization. A time-to-amplitude converter (TAC), and an analog-to-digital converter (ADC) on a PC board (PICOQUANT) were used to obtain the fluorescence decay histograms in 4096 channels with time increments of 2-5 ps/channel. The fluorescence decays were globally analyzed as a sum of exponentials with the time-resolved fluorescence analysis (TRFA) software. The quality of the fit was controlled by $\chi^2 <$ 1.1 and visual inspection of the residuals (55).

The relative fluorescence quantum yields (QYs) of the solution samples upon excitation at 410 and 515 nm were determined using a solution of perylene in toluene and rodamine 6G in water as a reference respectively. The molar extinction coefficients ($\varepsilon_A$) were determined by averaging the values obtained from the diluted solution prepared at three different concentrations ranging from $1\times10^{-6}$ to $1\times10^{-5}$ mol/L.

The film samples were prepared by spin-coating at a rotational speed of 1000 rpm from a solution in toluene of the compound (the concentration was 5 mg/mL) on a clean glass substrate. By this approach films with a thickness of about 100 nm could be obtained.

## RESULTS

### Triad 1 and polymer 1 in solution

***The excited states of triad 1 and polymer 1,*** in order to create a charge-transfer excited state as an effective mean to decrease the optical band gap, resulting in a bathochromic shift of the absorbance, we linked BODIPY 1 to ICZ 1 through the acetylenic π-spacers present on ICZ 1 (See Scheme 1), resulting in triad 1. The normalized UV-Vis absorption spectra of a diluted

solution in chloroform of ICZ 1, BODIPY 1 (53) and triad 1 and of ICZ 1, BODIPY 2 (53) and polymer 2 are illustrated in Fig. 1(a) and Fig. 1(b) respectively. The absorption spectrum of triad 1 in chloroform shows a maximum at 529 nm (See Fig. 1(a)), corresponding to a bathochromic shift of 32 nm or 0.15 eV compared to the parent BODIPY 1 for which the absorption has a maximum at 497 nm. With the goal to further shift the absorption spectrum of triad 1 towards longer wavelengths we synthesized a ICZ-π-BODIPY polymer (polymer 1) from BODIPY 2 and ICZ 1 (See Scheme 2) using a Sonogashira coupling. Compared to the triad a further broadening and a further red shift of the BODIPY centered absorption band to 611 nm were observed for a solution of polymer 1 in chloroform (See Fig. 1 (b)). This is red shift amounts to 75 nm (0.28 eV) compared to the parent BODIPY 2 with an absorption maximum at 536 nm. Compared to BODIPY 1 (See Fig. 1(a)) the shift is 114 nm or 0.46 eV. As the spectra of BODIPY 2 are quite strongly red shifted due to the presence of two iodine substituents it makes more sense to compare the spectra of polymer 1 to those of BODIPY 1 rather than to those of BODIPY 2. Furthermore the features of the absorption band of these complexes differ significantly from those of BODIPY 1 and BODIPY 2. The bands are broadened and the maximums no longer correspond to the 0-0 vibronic band as in their parent BODIPYs. For the triad 1 the 0-0 vibronic band can be attributed to the shoulder around 560 nm. However in contrast to triad 1 it is no longer possible to discern the position of the 0-0 vibronic transition from the features of the absorption band of polymer 1. As the maximum of the absorption bands of triad 1 and polymer 1 does not coincide with the 0-0 vibronic transition the red shift of the 0-0 transition is probably even larger than the shift of the maxima. For both triad 1 and polymer 1 similar features and a similar position of the maximum are observed in toluene, while in THF a small blue shift of the absorption band was

observed compared to chloroform or toluene. The estimated values of molar extinction coefficient at the absorption maximum of the triad 1 and polymer 1 in chloroform amount to $7.5\pm0.5\times10^4$ $M^{-1}cm^{-1}$and $7.0\pm0.5\times10^4$ $M^{-1}cm^{-1}$ at 530 and 611 nm respectively.

**Figure 1**

**Figure 2**

Excitation of the triad 1 at 515 nm in the BODIPY centered absorption band in toluene yields fluorescence with a maximum around 650 nm (see Fig. 2 (a)) and a fluorescence quantum yield of 8±1 %. In contrast to what is normally observed for BODIPYs (41,42,43,44,45,46,47,56) the transition is characterized by a large width of the absorption and emission bands and a large Stokes shift 0.44 eV. In chloroform and THF the emission maximum is shifted to 725 and 730 nm, and the fluorescence quantum yield ($\Phi_f$) is decreased to 0.5±0.1 and 0.20±0.05 %, respectively.

**Figure 3**

Upon excitation at 550 nm, i.e. in the BODIPY centered absorption band the fluorescence decay of triad 1 in toluene at 650 and 720 nm (Figure 3) could be fitted globally to a sum of two exponentials (Eq. 1) with amplitudes ($A_i$) and decay times ($\tau_i$) given in Table 1.

$$I(t) = \sum A_i \exp\left(-\,t/\tau_i\right) \qquad (1)$$

**Table 1**

Although the bi-exponential fluorescence decay suggests the presence of two different excited species the amplitudes of both components depend only marginally on the analysis wavelength. This suggests either that one of the excited species is not emitting or that both species have a similar emission spectrum. The average fluorescence decay time, $\langle\tau\rangle$, of the emission at 650 nm calculated using equation 2 amounts to 1.17 ns.

$$\langle\tau\rangle = \frac{\sum A_i \tau_i}{\sum A_i} \tag{2}$$

The fluorescence rate $\langle k_f \rangle$ constant calculated from the fluorescence decay time and the fluorescence quantum yield using equation 3 amounted to $6.9 \times 10^7$ $s^{-1}$ which is a three to four times smaller than the values generally obtained for a BODIPY in apolar solvents (40,41,42,43,44,45,46,47,53).

$$\langle k_f \rangle = \frac{\Phi_f}{\langle\tau\rangle} \tag{3}$$

In chloroform and THF the fluorescence decays had to be analyzed as a sum of three exponentials. However, for the component with the shortest decay time a decay time of only 20 ps was recovered which is beyond the time resolution of the set-up. As this component was no longer observed when the sample in chloroform was excited at 410 nm (See Data S1) it was attributed to scattered light and its presence was neglected in the further data analysis which yielded the values of amplitudes and decay time shown in table 1. Upon increasing the solvent polarity from toluene over chloroform to THF both decay times as well as the average decay time calculated for the emission at 650 nm, which is, in contrast to what is observed in toluene, very close to $\tau_1$, decrease. The amplitude of the component with the longest decay time is

significantly smaller than in toluene and shows a small decrease upon increasing the emission wavelength from 650 to 720 nm. Also the value of $<k_f>$ is decreased upon increasing the solvent polarity (See table 1).

**Figure 4**

As illustrated in Fig. 4 (a) excitation of the polymer 1 at 600 nm, in the BODIPY centered absorption band, yields in toluene a fluorescence spectrum with a maximum around 680 nm. The fluorescence quantum yield obtained upon excitation at 515 nm amounts to 5.5±0.5 % (Fig. 4 (a)). In chloroform and THF the emission maximum is shifted to 700 nm and 705 nm respectively, while the fluorescence quantum yield for excitation at 515 nm has decreased to 1.2±0.1 and 0.49±0.05 % respectively.

**Table 2**

Upon excitation at 635 nm the fluorescence decay of polymer 1 in toluene at 670 and 720 nm could be analyzed as sum of two exponentials (Table 2). While the value of short decay time, $\tau_1$, is close to that observed for triad 1, the long decay time, $\tau_2$, is significantly smaller. The amplitudes of both decay times are close to those observed for triad 1 and do not depend upon the emission wavelength while also the value of $<k_f>$ is close to that observed for triad 1. In chloroform and THF the fluorescence decays have to be analyzed as a sum of three exponentials while the shortest decay time of respectively 22 and 9 ps is much shorter than the time resolution of the set-up. As in analogy to triad 1, this component was no longer observed when the sample in chloroform was excited at 410 nm (See Data S1) it was attributed to scattered light and its presence was neglected in the further data analysis (See table 2). Upon

increasing the solvent polarity for toluene over chloroform to THF the short decay time, $\tau_1$, as well as the average decay time calculated for the emission at 670 nm, which is, in contrast to what is observed in toluene, very close to $\tau_1$, decrease while the long decay time changes much less. In analogy to what was observed for triad 1 the amplitude of the component with the longest decay time is significantly smaller than in toluene and shows a small decrease upon increasing the emission wavelength from 670 to 720 nm. Also the value of $<k_f>$ is decreased upon increasing the solvent polarity (see table 2).

***The intramolecular energy transfer in triad 1 and polymer 1,*** figure 2 (b) shows the fluorescence spectrum of triad 1 in toluene upon excitation at 410 nm in the $S_0 \rightarrow S_2$ absorption band (the $S_0 \rightarrow S_1$ transition on the ICZ moiety). This spectrum displays a maximum around 650 nm and a fluorescence quantum yield of 9±1 %, which are both comparable to the data obtained for direct excitation of the BODIPY moiety. Furthermore around 430-440 nm a very weak secondary maximum with a fluorescence quantum yield of 0.08±0.02 % is observed. The latter is attributed to residual emission of the ICZ moiety and suggests incomplete quenching of the ICZ emission by the BODIPY. As the fluorescence quantum yield of free ICZ 1 in toluene amounts to 30±3 %, this means according to Eq. 4 that the quenching is at least for 99.7 % efficient.

$$\Phi_q = 1 - {}^{\Phi_{DA}}/_{\Phi_D} \qquad (4)$$

In the equation above $\Phi_{DA}$ is the fluorescence quantum yield of the ICZ emission in the triad or polymer, $\Phi_D$ the fluorescence quantum yield of ICZ 1 and $\Phi_q$ the fluorescence quantum yield of quenching. As the fluorescence quantum yield of the long wavelength emission (650

nm) is within experimental error the same for excitation at 410 and 510 nm, the quenching can be attributed nearly exclusively to energy transfer. This is confirmed by coincidence of the absorption spectrum of triad 1 in toluene with the excitation spectrum of the emission at 700 nm in toluene (See Data S2, Figure S2 (a)). If a significant fraction of the excited ICZ moieties were quenched by another process the relative intensity of the band around 400 nm (compared to that around 600 nm) should be smaller in the excitation than in the absorption spectrum. Also in chloroform and THF the emission spectra obtained upon excitation at 410 nm consisted of a long wavelength band and a band around 430-440 nm. The long wavelength band was, identical to that obtained upon excitation at 515 nm and was attributed to a transition mainly located on BODIPY moiety while the short wavelength band was attributed to a transition localized on the ICZ 1 moiety, considering the similarity of its features and position with those of the emission spectrum of ICZ derivatives. The short wavelength band is decreased in intensity in chloroform and THF but to a much smaller extent than the long wavelength band. In chloroform and THF the quenching of ICZ emission occurs with an efficiency of around 98.7 %.

Figure 4 (b) shows the emission spectra of polymer 1 obtained in toluene upon excitation at 410 nm, *i.e.* in the $S_0 \rightarrow S_1$ absorption band of the ICZ moiety. The long wavelength band of this emission spectrum has a maximum around 680 nm and a fluorescence quantum yield of 5.2±0.5 %, comparable to those observed for direct excitation of the BODIPY moiety. Furthermore around 430-440 nm a very weak secondary maximum attributed to residual emission of the ICZ moiety is observed with a fluorescence quantum yield of 0.4±0.04 % (Fig. 4 (b)). As in triad 1 these data suggest incomplete quenching of the ICZ emission by the BODIPY moiety The quantum yield of fluorescence quenching amounts to at least 98.7 %,

which is slightly less than found for triad 1. In chloroform and THF similar results were obtained, corresponding to a fluorescence quenching efficiency of 98.3 and 99.1% respectively. When comparing the ratios of the amplitude of the 400 nm and 600 nm band in the absorption spectrum and the excitation spectrum of the fluorescence at 720 nm (See Data S2, Figure S2 (b)), both obtained in toluene, one observes that at 400 nm this ratio is 18±2 % smaller for the excitation spectrum relative to the absorption spectrum. This means that the 18±2 % of the quenching does occur by another process than energy transfer to the BODIPY centered transition.

**Figure 5**

In order to obtain more information on the energy transfer the fluorescence decay of the ICZ-centered emission was determined by single photon timing (SPT) in the triad 1, polymer 1, and the model compound ICZ 1. The ICZ-centered state was excited at 410 nm and the decay of its emission was recorded at 460 nm (See Fig. 5). The fluorescence decays were analyzed as a sum of exponentials (Eq. 1). For ICZ 1 the fluorescence decay could be analyzed as a sum of two exponentials (Table 3) for both solvents. One should note that the data in Table 3 indicate that the slow decaying component, corresponding to $A_2\tau_2/(A_1\tau_1 + A_2\tau_2)$, contributes to 97 and 94 % of the total emission in toluene and chloroform respectively. A triple exponential decay was required to fit the data for triad 1 and polymer 1 (Table 3). For triad 1 and polymer 1 the recovered values of the shortest decay time, $\tau_1$, range from $1.9\text{x}10^{-2}$ to $7.4\text{x}10^{-2}$ ns, which is very close to or below the time resolution of the set-up ($5\text{x}10^{-2}$ ns). A tri-exponential decay would mean that there are three distinct excited species. However neither for triad 1 nor for polymer 1 there is an obvious reason to have three distinct excited state populations decaying

with a different rate. This means that the triple exponential decay most likely represents a continuous distribution of decay times roughly ranging from $\tau_1$ to $\tau_3$. Although in this approach it is not possible to attribute a physical meaning to the individual decay times, these parameters however can be used to calculate the average decay time $<\tau>$ (See Eq. 2) of the excited state of the ICZ moiety in triad 1 and polymer 1

**Table 3**

The range of decay times is situated at smaller values than the average decay time of the model compound ICZ 1. This observation, which is reflected in values of the average decay times, suggests that the ICZ fluorescence is quenched by the BODIPY or DPP moieties. As analysis of the stationary photoluminescence data already suggested that this quenching is nearly exclusively due to energy transfer from the excited state situated on the ICZ moiety to a state mainly situated on the BODIPY moiety, the distribution of decay times most probably represents a distribution of rate constants for energy transfer (vide infra). The recovered values of the amplitudes suggest that the distribution is biased strongly towards the shorter decay times, i.e. larger rate constants for energy transfer for triad 1 and polymer 1. Similar to Eq. 4, the efficiency of quenching of the ICZ fluorescence by a transition mainly situated on the BODIPY or DPP moiety can be estimated by Eq. 5.

$$\Phi_{q\tau} = 1 - \left\langle \tau_{DA} \right\rangle \Big/ \left\langle \tau_{D} \right\rangle \tag{5}$$

$\Phi_{q\tau}$ is the quenching efficiency. $<\tau_D>$ represents the amplitude-weighted average fluorescence decay time recorded from a solution of ICZ 1, and $<\tau_{DA}>$ is the amplitude-

weighted average fluorescence decay time obtained for the ICZ centered emission of triad 1, or polymer 1. In the same approach the average rate constant for quenching $<k_{q\tau}>$ is given by Eq. 6.

$$\left\langle k_{q\tau} \right\rangle = \frac{1}{\left\langle \tau_{DA} \right\rangle} - \frac{1}{\left\langle \tau_{D} \right\rangle} \tag{6}$$

The values of $<k_{q\tau}>$ obtained in this way range from $1.6x10^9$ (chloroform) to $2.2x10^9$ $s^{-1}$ (toluene) and from $1.1x10^9$ (toluene) to $4.8x10^9$ $s^{-1}$ (chloroform) for triad 1 and polymer 1 respectively. Based on the values of $\langle\tau\rangle$ obtained from a solution of ICZ 1, rate constants ($k_d = 1/<\tau_D>$) of $1.6\times10^8$ $s^{-1}$ and $2.3\times10^8$ $s^{-1}$ can be estimated for the decay of the singlet excited state of ICZ 1 in absence of quenching in toluene and chloroform respectively. Using the quenching efficiencies obtained by Eq. 4, the quenching rate constants $<k_{q,stat}>$ can be estimated using equation 7.

$$\left\langle k_{q,stat} \right\rangle = \frac{\Phi_q}{1-\Phi_q} * \frac{1}{\left\langle \tau_{D} \right\rangle} \tag{7}$$

The values of $<k_{q,stat}>$ obtained in this way range from $5.3x10^{10}$ (toluene) to $1.7x10^{10}$ $s^{-1}$ (chloroform) and from $1.2x10^{10}$ (toluene) to $1.3x10^{10}$ $s^{-1}$ (chloroform) for triad 1 and polymer 1 respectively. The quenching efficiencies for triad 1 and polymer 1, estimated on the basis of the time-resolved fluorescence experiments ($\Phi_{q\tau}$), are smaller (5 to 10 %) than those estimated from the fluorescence quantum yields (Eq. 4) in both toluene and chloroform while on the other hand the values of $<k_{q,stat}>$ determined form Eq. 7 are about one order of magnitude larger than those of $<k_{q\tau}>$ determined form Eq. 6. A reason for this discrepancy is that the way the average decay time is calculated emphasizes long decay times and hence the tail of the

distribution of the quenching rate constants. This means that such procedure to estimate an average decay time can only be used if the different decay times do, contrary to the present case, differ less than one order of magnitude. Furthermore the values found for the shortest decay time, $\tau_1$, are subject to a large relative error as they are close to or beyond the time resolution of the set-up. One cannot exclude that at short times the decay is faster than the time-resolution of our set-up ($5.0 \times 10^{-2}$ ns) and that static quenching occurs (57,58). This could also explain the large discrepancy between the values of $<k_{q\tau}>$ found for triad 1 and polymer 1 in the two solvents.

## Polymer 2 in solution

***The excited states of polymer 2,*** in the previous sections the use of a BODIPY as an electron accepting building block in the synthesis of the D-A conjugated systems has been investigated. It has been demonstrated that diketopyrrolopyrrole (DPP) is also a good co-monomer for thiophene based D-A polymers (48,51,59) and therefore we synthesized an alternating copolymer (polymer 2) of DPP and ICZ 1 through the use of the acetylenic π-spacers.

Figure 6 shows the normalized absorption spectra of a dilute solution in chloroform of ICZ 1, DPP 1 and polymer 2. Polymer 2 shows an absorption maximum at 505 nm with a molar extinction coefficient (for one ICZ-DPP dyad) of ~ $4.5 \times 10^4$ $M^{-1}cm^{-1}$, corresponding to a bathochromic shift of 25 nm (0.13 eV) relative to the parent DPP 1. As previously described, the absorption band at 426 nm is attributed to the ICZ moiety. In analogy to the observations made for the triad and polymer 1 a blue shift by ~ 7 nm of the absorption band is observed in THF.

## Figure 6

The normalized photoluminescence (PL) spectrum of polymer 2 in toluene upon excitation at 515 nm, i.e. in the DPP centered band, shows fluorescence with a maximum around 577 nm, corresponding to a Stokes shift of 72 nm (0.31 eV), and a shoulder around 625 nm. The distance between both bands is 0.16 eV which can correspond with the frequency of a carbon - carbon vibration of the ring. This would indicate that the bands at 577 and 625 nm correspond to the 0-0 and 0-1 vibronic transitions. The fluorescence quantum yield ($\Phi_f$) amounts to 65.2 % in toluene. In chloroform and THF the maximum of the fluorescence spectrum obtained upon excitation at 515 nm shifts to 700 and 675 nm while the fluorescence quantum yield is decreased to 3.9±0.4 and 1.9±0.2 % respectively and the vibrational fine structure is lost.

Upon excitation at 488 nm, i.e. in the DPP centered absorption band the fluorescence decay of polymer in toluene at 600 (Fig. 8), 650 and 700 nm could be fitted globally to a sum of two exponentials (Eq. 1) with amplitudes ($A_i$) and decay times ($\tau_i$) given in Table 4.

## Figure 7

## Figure 8

Although the bi-exponential fluorescence decay suggests the presence of two different excited species the amplitudes of both components depend only marginally on the analysis wavelength. This suggests either that one of the excited species is not emitting or that both species have a similar emission spectrum. The average fluorescence decay time, $\langle\tau\rangle$, of the emission at 650 nm calculated using equation 2 amounts to 2.42 ns. The fluorescence rate constant $\langle k_f \rangle$ calculated from the fluorescence decay time and the fluorescence quantum yield

using equation 3 amounted to $2.7x10^8$ $s^{-1}$, which is of the order of magnitude of the values observed for DPP (60).

In chloroform and THF the fluorescence decays have to be analyzed as a sum of four exponentials while the shortest decay time of respectively 13 and 12 ps is much shorter than the time resolution of the set-up. In analogy to triad 1 and polymer 1, this component, which was not observed upon excitation at 410 nm (See S1), was attributed to scattered light. Hence its presence was neglected in the further data analysis (Table 4). Upon increasing the solvent polarity from toluene over chloroform to THF the decay times $\tau_1$ and $\tau_2$ decrease, in analogy to the results obtained for triad 1 and polymer 1. However in contrast to what was observed for triad 1 and polymer 1 a third component with a shorter decay time ($\tau_3$) is necessary to obtain a good fit. In analogy to what was observed for triad 1 and polymer 1 the amplitude of the component with the longest decay time ($\tau_2$) is significantly smaller than in toluene and shows a small decrease upon increasing the emission wavelength from 600 to 700 nm. Also the value of the average decay time $<\tau>$, calculated for the emission at 600 nm and $<k_f>$ are decreased upon increasing the solvent polarity (Table 4).

***The intramolecular energy transfer in polymer 2,*** upon excitation at 410 nm (See Fig. 7 (b)) the fluorescence quantum yield for emission from the DPP moiety amounts to 47±5 % in toluene which is smaller than the value (65.2±0.065) found upon excitation at 515 nm, while that of the ICZ emission amounts to 3.6±0.4 %. According to equation 4 this means that the ICZ emission is quenched for at least 88.2 %, which is about 10 % smaller than the values found for triad 1 and polymer 1, probably by energy transfer to a DPP centered excited state. When comparing the ratios of the amplitude of the 400 nm and 600 nm band in the absorption

spectrum and the excitation spectrum of the fluorescence at 650 nm (See Data S2, Figure S2 (c)), both obtained in toluene, one observes that at 400 nm this ratio is 37±4 % smaller for the excitation spectrum relative to the absorption spectrum. If all quenching would occur by energy transfer this ratio should only by 12±4 % smaller for the excitation than for the absorption spectrum (as the quenching efficiency is 88 %). This means that the 26±3 % of the ICZ moieties are quenched by another process than energy transfer to the DPP centered excited state or that 26/0.88 = 30±3 % of the quenching does occur by another process than energy transfer to the DPP centered transition. This agrees with the observation that the fluorescence quantum yield of the DPP centered emission is 18±2 % smaller upon excitation at 410 nm compared to excitation at 515 nm. In order to obtain more information on the energy transfer the fluorescence decay of the ICZ-centered emission of polymer 2 was determined by single photon timing (SPT). The ICZ-centered state was excited at 410 nm and the decay of its emission was recorded at 460 nm (See Fig. 5). The fluorescence decays were analyzed as a sum of three exponentials (Eq. 1) yielding the results shown in Table 3. While for the triad 1 and polymer 1 the component with the shortest decay time ($\tau_1$) had a decay time very close to or below the time resolution of the set-up $\tau_1$ was three to ten times larger for polymer 2. Furthermore this component had a considerably smaller amplitude ($A_1$). As in analogy to triad 1 and polymer 1 there is no obvious reason to have three distinct excited state populations decaying with a different rate the triple exponential decay most likely also represents a continuous distribution of decay times roughly ranging from $\tau_1$ to $\tau_3$. As for triad 1 and polymer 1 the fit parameters can however be used to calculate the average decay time $<\tau>$, the efficiency of the quenching ($\Phi_{q\tau}$) and the average quenching rate constant ($<k_{q\tau}>$) using Eq. 2, 5 and 6 respectively (*cfr. supra*). In this way values of $\Phi_{q\tau}$ and $<k_{q\tau}>$ of 58 % and 59 %, and

$2.2x10^8$ $s^{-1}$ and $3.3x10^8$ $s^{-1}$ were obtained in toluene and chloroform respectively (Table 3). Considering the stationary fluorescence data this quenching is to a large extent due to energy transfer from the excited state situated on the ICZ moiety to a state mainly situated on the BODIPY moiety. In contrast to what was observed for triad 1 and polymer 1 where the recovered values of the amplitudes suggest that the distribution is biased strongly towards the shorter decay times, i.e. larger rate constants for energy transfer, the distribution is more symmetric and uniform for polymer 2. Furthermore the recovered values of the decay times recovered for polymer 2 are significantly longer than those recovered for triad 1 or polymer 1. This is reflected in the value of $\Phi_{q\tau}$ which are 40 % smaller than those found for triad 1 and polymer 1 while the values of $<k_{q\tau}>$ are five to fifteen times smaller than those found for triad 1 and polymer 1. The quenching rate constant $<k_{q,stat}>$, calculated using Eq. 7 amounts to $1.2x10^9$ $s^{-1}$ in toluene which is an order of magnitude smaller than the values of $<k_{q,stat}>$ found for triad 1 and polymer 1 in toluene. In analogy to what was observed for triad 1 and polymer 1 the value estimated for $<k_{q\tau}>$ for polymer 2 in toluene is five times smaller than that estimated for $<k_{q,stat}>$, hence also the value of $\Phi_{q\tau}$ in toluene is 30 % smaller than that of $\Phi_q$.

## Films of triad 1 and Polymer 1

### Figure 9

As the spectra of conjugated polymers often differ significantly in neat films (used in OLEDs or OPVs) when compared to a dilute solution, we also investigated the spectroscopic properties of triad 1 and polymer 1 in a thin spin-coated film. Figure 9 illustrates normalized absorption spectra obtained from a solution and a spin-coated film of the triad 1 (a) and those

of the polymer 1 (b). In contrast to the solution samples, a broader absorption spectrum with the maximum shifted to 621 nm, which corresponds to a shift of 0.35 eV compared to a solution in toluene, observed for the film of triad 1. Furthermore this band has a tail extending to 1000 nm. In addition a shoulder between 550 and 570 nm is observed. The film of polymer 1 has no shift of the absorption peak. The spectrum is only slightly broadened compared to the solution which could be attributed to an increased degree of disorder (61).

**Figure 10**

The fluorescence spectrum of the films of triad 1 and polymer 1 consists of a broad band with maximum at respectively 708 and 740 nm (See Fig. 10). Compare to a solution in toluene the emission is shifted over 58 nm (0.16 eV) and 60 nm (0.15 eV) for triad 1 and polymer 1 respectively. In the film the Stokes shift amounts to 87 nm (0.25 eV) and 129 nm (0.35 eV) for triad 1 and polymer 1 respectively.

## DISCUSSION

**The properties of the lowest excited state** For triad 1 and polymer 1 both the shift of the 0-0 transition of the long wavelength absorption band compared to respectively BODIPY 1 and 2 as well as the significant increase of the width of this band suggest a partial delocalization of the lowest excited singlet state over the ICZ moiety. The small blue shift of the absorption band in THF can be attributed to decreased polarizability of the solvent (56). The absence of a red shift of the absorption maximum upon increasing the solvent polarity suggests that the ground state has little to no permanent dipole moment. The less intense absorption signal at 430 nm can be

attributed to a transition residing mainly on the ICZ chromophore. The much smaller red shift of this transition compared to the parent ICZ is probably due to the fact that it is oriented along the short axis (6-12 direction) of the ICZ and hence less influenced by the conjugation.

The increase of the Stokes shift as well as the major red shift of the emission of triad 1 and polymer 1 upon increasing the solvent polarity suggest a significant dipole moment and hence charge transfer character of the excited state, $ICZ^{\delta+}$-$BODIPY^{\delta-}$ (Scheme 5) (56). A similar behavior could be observed when BODIPY dyes are conjugated to an electron donor such as in 2-anilinosubstituted BODIPY (40). The Stokes shift observed for polymer 1 in toluene (0.21 eV) is much smaller than the one observed for the triad (0.44 eV) which suggests a less extensive change in geometry upon excitation. This correlates with more extensive delocalization leading to a reduced exciton phonon coupling. One should note that for polymer 1 the solvent dependence of the Stokes shift and the emission maximum are smaller than observed for triad 1 suggesting a smaller excited state dipole moment. As each BODIPY is now conjugated on both sides to an ICZ moiety, charge transfer from both ICZ moieties to the BODIPY could lead to a quadrupolar rather than a dipolar structure.

**Scheme 5**

The analysis of the fluorescence decays of the long wavelength emission shows the presence of two excited species. Either one of those species is non emitting or both species have a nearly identical emission spectrum in toluene as the values of amplitudes of both components of the decay are within experimental error identical at 650 (for triad 1) or 670 nm (for polymer 1) and 720 nm. If one assumes a single emitting species the interconversion between both species is reversible leading to a bi-exponential decay (62). As photo-excitation (or energy

transfer from the ICZ centered excited state (*cfr. infra*)) will form the fluorescent species the rate for interconversion can be approximated by the inverse of the short decay time, $\tau_1^{-1}$, while the inverse of the long decay time, $\tau_2^{-1}$, is a weighted average of the inverse decay times of both species (62,63,64). In this framework, the ratio of the pre-exponential factors then reflects to some extent the position of the equilibrium between both states. A likely candidate for the nonfluorescent species is a completely charge separated state (electron transfer state) as $ICZ^{+}$-$BODIPY^{-}$ (Scheme 5) with a radical cation on the ICZ moiety and a radical anion on the BODIPY moiety. Such process was also observed for a bisthiophene substituted peryleneimide (65) and rigid perylene end-capped pentaphenylenes (66), although due to a stronger interaction between the electron donor and acceptor this CT-state was still emitting in these systems. Due to the spatial separation and limited overlap of the wavefunctions of the radical cation and the radical anion such state will have a very small transition dipole towards the ground state (67,68). It will furthermore be more stabilized than the partially charge separated state upon increasing the solvent polarity which could explain why the amplitude of the slow decaying component decreases strongly upon increasing the solvent polarity. The decrease of the long decay time, $\tau_2$, upon increasing the solvent polarity is hence due to the stabilization of the charge transfer state, decreasing the energy difference with the ground state and the increase of the reorganization energy (68,69,70,71). While for triad 1 the quenching of the ICZ-emission leads nearly exclusively to the formation of the emitting partial charge separated state, $ICZ^{\delta+}$- $BODIPY^{\delta-}$, the excitation spectra suggest that in polymer 1 the quenching of the ICZ occurs partially by another mechanism, which could be the direct formation of the fully charge separated state, $ICZ^{+}$- $BODIPY^{-}$.

The red shift of the long wavelength absorption band and the fluorescence spectrum in toluene of polymer 2 suggests that, in analogy to triad 1 and polymer 1, the orbitals involved in this transition are to some extent delocalized between the ICZ and the DPP moieties, although to a smaller extent than in polymer 1. The less extensive delocalization, suggested by the smaller red shift of the absorption band versus that of DPP 1, is confirmed by the observation that while the average fluorescent rate constant of triad 1 and polymer 1 is much smaller than that of the corresponding BODIPY model compounds that of polymer 2 is close to the values that can be calculated for a diketopyrrolo-pyrrole (60). The broadening of the DPP centered absorption band and the better vibrational fine structure of the fluorescence spectrum (compared to the absorption spectrum) suggest a change in molecular geometry, *e.g.* planarization, upon excitation. The blue shift of the long wavelength absorption band in THF can, in analogy to triad 1 and polymer 1, be attributed to decreased polarizability of THF compared to chloroform or toluene (56). The increase of the Stokes shift as well as the major red shift and loss of vibrational fine structure of the emission of polymer 2 upon increasing the solvent polarity suggest the formation of an excited state with a significant dipole moment and charge transfer character (56). In analogy to the results obtained for triad 1 and polymer 1 the analysis of the time-resolved fluorescence experiments suggests that this state with a partial charge transfer is in equilibrium with a non-fluorescent electron transfer state, $ICZ^{+}$- $DDP^{-}$ (Scheme 5). In analogy to what is observed for polymer 1, the fluorescence excitation spectra show that for polymer 2 the quenching of the ICZ emission leads only partially to the population of the fluorescent partial charge separated state, $ICZ^{\delta+}$-$BODIPY^{\delta-}$. This could suggest that for polymer 2 this fully charge separated state, $ICZ^{+}$- $DDP^{-}$, can also be populated

directly by the quenching of the ICZ centered excited state. The larger amplitude of the component with decay time $\tau_2$ indicates that this electron transfer state is less stabilized versus the fluorescent partial charge transfer state than in triad 1 or polymer 1 (62,63,64). The more complex decays observed in chloroform or THF compared to triad 1 or polymer 1, are probably due to the presence of oligomers with different chain lengths. One should note that also a bisthiophene substituted perylenimide yielded two different electron transfer states in polar solvents (65).

**The intramolecular energy transfer** For triad 1, polymer 1, and polymer 2 we observed that the rate constant for energy transfer from the ICZ centered excited sate to the excited state centered on the BODIPY or DPP moiety determined for stationary fluorescence experiments, $<k_{q,stat}>$, is always significantly larger than that obtained from time-resolved experiments, $<k_{q\tau}>$. As the way the average fluorescence decay time $<\tau>$ is calculated emphasizes long decay times and hence the tail of the distribution of the quenching rate constants, the values of $<k_{q\tau}>$ are probably underestimated. For triad 1 and polymer 1 the inability to measure accurately components of the decays with a decay time less than the time resolution of our set-up for SPT (static quenching) (57,58) can lead to a further underestimation of $<k_{q\tau}>$. This argument does however not hold for polymer 2 where the shortest decay times of 270 and 210 ps in toluene and chloroform respectively are clearly much larger than the time resolution of the SPT set-up. In spite of this discrepancy it is remarkable that both approaches yield for polymer 2 values of the rate constant for quenching of the ICZ emission that is an order of magnitude smaller found for triad 1 or polymer 1. The much smaller values of $<k_q>$ and $<k_{q,stat}>$ observed for polymer 2 were initially unexpected as the overlap between the long

wavelength absorption and the fluorescence of the ICZ chromophore is similar for the three compounds.

When an excited state (in this case the BOPDPY centered partial charge transfer state) is formed starting from another excited state (in this case the ICZ-centered excited state) by energy transfer or complex formation (62,63,64) one expects that the fluorescence decay of the former one can be described by a difference of two exponentials with equal amplitude, i.e. the fluorescence decay should be characterized by a growing-in. However upon excitation at 410 nm the fluorescence decay of the emission of neither $ICZ^{\delta+}$-$BODIPY^{\delta-}$ (triad 1 or polymer 1) nor $ICZ^{\delta+}$-$DDP^{\delta-}$ (polymer 2) contained components with a negative amplitude. While for triad 1 and polymer 1 the failure to observe such component could be attributed to the fact that its decay time (*i.e.* the growing in time constant) is beyond the time resolution of the set-up, this argument does not hold for polymer 2. At least for the latter compound the failure to observe a growing in of the fluorescence is possibly due to the overlap of the absorption spectra of the ICZ-centered excited and the DPP centered partial charge transfer excited state or the formation of the partial charge transfer state (corresponding to the DPP centered emission) from the fully charge separated state (dashed lines in scheme 5). One should note that also in other systems characterized by intramolecular excitation transfer (72,73) no component with negative amplitude could be observed for the acceptor emission.

In order to get further insight in the values of $<k_{q\tau}>$ and $<k_{q,stat}>$ (which we attributed to energy transfer), we estimated the rate constants for Förster type energy transfer (74,75,76) between

the transition centered on the ICZ chromophore and that centered on the BODIPY or DPP chromophore. The characteristic distance for energy transfer, $R_0$, is given by Eq. 8,

$$R_0 = 0.021085\left(J\kappa^2 n^{-4}\Phi_f^0\right)^{1/6} \quad (8)$$

where J is the spectral overlap integral, κ the orientation factor, n the refractive index of the medium, (which is 1.496 for toluene and 1.446 for chloroform), and $\Phi_f^0$, is the fluorescence quantum yield of the ICZ chromophore (0.30±0.03 and 0.16±0.02 in toluene and chloroform respectively). The spectral overlap integral J in $M^{-1}cm^{-1}nm^4$ is given by Eq. 9,

$$J = \int \varepsilon_A(\lambda) F_D(\lambda) \lambda^4 d\lambda \quad (9)$$

where $\varepsilon_A(\lambda)$ is the molar extinction coefficient of the acceptor ($M^{-1}cm^{-1}$), $F_D(\lambda)$ is the area normalized fluorescence spectrum of the donor ($nm^{-1}$). The orientation factor κ is given by Eq. 10,

$$\kappa = \cos\alpha - 3\cos\Theta_D \cos\Theta_A \quad (10)$$

where α is the angle between the transition dipoles of donor and acceptor, and $\Theta_A$ and $\Theta_D$ are the angles between the transition dipoles of each the donor and acceptor and the vector linking their center. For the triad 1 and polymer 1, α, $\Theta_A$ and $\Theta_D$ amount to 20°, 22° and 42° respectively yielding -1.13 and 1.27 for κ and $\kappa^2$ (Fig. 11).

**Figure 11**

For polymer 2 $\alpha$, $\Theta_A$ and $\Theta_D$ amount to 43°, 83° and 40° based on the orientation of the transition dipole in the DPP chromophore as established by Mizuguchi et al. (see Data S3, Fig. S3) (59). This approach yielded 0.45 and 0.20 for $\kappa$ and $\kappa^2$ for polymer 2 (Fig. 11). In these estimations a planar structure was assumed for the molecules. Deviations from this planar structure will lead to a decrease of $\kappa^2$ as discussed below. Using equation 8 to 10 the values of $R_0$ given in Table 5 are obtained.

We can also write the equation for $k_{Förster}$, the rate constant for energy transfer by the Förster mechanism as

$$k_{Förster} = k_d \, R_0^6 / R^6 \qquad (11)$$

Where $k_d = 1/\langle\tau_D\rangle$ ($s^{-1}$) is the rate constant for the decay of the fluorescence of ICZ 1, and R the distance between the centers of the donor and the acceptor. Using values of $1.60 \times 10^8$ $s^{-1}$ and $2.28 \times 10^8$ $s^{-1}$ for $k_d$ in respectively toluene and chloroform and values of 1.26 and 1.46 nm for R (for respectively triad 1 or polymer 1 and polymer 2) we obtain the values of $k_{Förster}$ given in Table 5. The values of R were determined from the structures in scheme 1, 2 and 3.

**Table 5**

First of all, we note that the calculated values of $k_{Förster}$ are systematically about a factor 10 to 40 larger than the fastest rate constants for quenching of the ICZ emission observed experimentally (which we put equal to $\tau_1^{-1}$) in the time resolved experiments. A similar discrepancy (except for triad 1 in $CHCl_3$) is observed when we consider the values $\langle k_{q,stat} \rangle$ inferred from the stationary fluorescence experiments using Eq. 4 and 7. The analysis of the

nature of the fluorescence decays indicates that besides a large fraction of molecules with a fast decay time of the ICZ emission there is always a small fraction present with a decay time close to that of unquenched ICZ. While for triad 1 and polymer 1 this fraction is no more than a few percent, and could perhaps be attributed to an impurity not containing a BODIPY chromophore, this fraction amounts to 35 to 40 % for polymer 2. Considering the fact that the NMR spectra do not suggest the presence of such an impurity for any of the three compounds, it is highly unlikely that the fraction of molecules of polymer 2 with a long fluorescence decay time corresponds to an impurity. The latter argument as well as the systematic difference between the values of the calculated rate constants, $k_{Förster}$ and those of the experimentally estimated rate constants, $\tau_1^{-1}$ or $<k_{q,stat}>$, which mutually agree, indicates that the discrepancy is not due to the experimental uncertainty or artifact and must have a more fundamental reason.

Equations 7 to 10 are based on a point dipole approximation for the transition dipoles of the donor and acceptor. It has been shown that when the size of the chromophores is no longer negligible compared to the distance between the centers of donor and acceptor, the Coulomb matrix element, which is the perturbation responsible for Förster type energy transfer, is overestimated (77,78,79,80,81) by this point dipole approximation. If, for example a center to center distance of 1 nm is used, the matrix element is overestimated by about a factor three which means that the rate constant, which is proportional to the square of this matrix element, is overestimated by a factor of ten. Taking this overestimation into account, the values of $k_{q,Förster}$ estimated from the absorption spectra of the transitions centered at BODIPY or DPP and the emission spectra of the ICZ centered transitions, become similar to the experimental values of $\tau_1^{-1}$ or $<k_{q,stat}>$. Furthermore one should note that the ratio of the values of $k_{q,Förster}$ for

triad 1 or polymer 1 to those of polymer 2 resembles the ratio of the values of $\tau_1^{-1}$ or $<k_{q,stat}>$ of triad 1 or polymer 1 to those of polymer 2. When considering the calculations for $k_{q,Förster}$ it is clear that this difference is mainly due to ratio of the value of $<\kappa^2>$ for triad 1 or polymer 1 to that of polymer 2.

One has also to take into account that the energy transfer is not purely driven by Coulomb interaction (74,75,76), but that configuration interaction with charge transfer configurations (82,83,84) as well as exchange interactions (85) also provide a contribution to the rate constant for energy transfer. The latter contributions require orbital overlap between both chromophores which will occur mainly through the acetylenic linker (through-bond) (83,86). Although the spectral shift of the BODIPY centered band in triad 1 or polymer 1 and the DPP centered band in polymer 2 versus respectively bands of the parent BODIPY or DPP molecules, suggests orbital interaction between both chromophores, the energy transfer rates and their difference between triad 1 or polymer 1 and polymer 2 are in good agreement with those predicted for Förster transfer when the point dipole approximation is replaced by a more realistic extended dipole approximation (82,83,84). This agrees with earlier observations for intramolecular energy transfer between porphyrines connected by a phenanthroline (72). If other transfer mechanisms would have a major contribution this would only lead to a larger discrepancy between the observed and calculated rates for energy transfer. Also the delocalization of the wavefunctions of the ICZ and BODIPY or DPP chromophores over the acetylenic linkers or beyond would lead to a limited enhancement of the coupling and hence to an increase of $k_{Förster}$ which would increase the discrepancy with the experimental results (66,87).

For triad 1, polymer 1 and polymer 2 the analysis of the fluorescence decays showed a distribution of decay times of the ICZ emission reflects a distribution of rate constants for energy transfer. For energy donor and acceptor linked by a rigid acetylenic spacer, rotation of the donor and acceptor around this linker is the only structural parameter for which a relatively broad distribution can be expected. In triad 1 and polymer 1 a rotation of the BODIPY moiety around the acetylenic spacer will only lead to modest changes in $\alpha$ and $\Theta_A$ and hence in $\kappa^2$ (see Fig. 11). However, in polymer 2 a rotation of the DPP moiety around the acetylenic spacer (see Fig. 11) will lead to major changes in $\alpha$ and hence in $\kappa^2$. Equation 10 predicts (keeping $\Theta_D$ at 83 ° and $\Theta_A$ at 40° respectively) that $\kappa^2$ and hence $k_{q,Förster}$ would equal zero for polymer 2 when $\alpha$ would become equal to 73°. Furthermore, one should take into account that for all compounds leaving the coplanar configuration would also reduce the orbital overlap between the ICZ and BODIPY (or DPP) moieties and hence the contribution of exchange or charge transfer interactions to the rate constants for energy transfer.

**Films of triad 1 and Polymer 1** The red shift of the maximum of the absorption band of triad 1 in the film compared to a solution in toluene suggests exciton interaction in a J-type packing or a highly disordered H-type packing (88,89,90). The origin of the shoulder at 560 nm is less clear. As there is no longer a maximum observed around 529 nm, where the maximum is observed in toluene, it is unlikely that this peak corresponds to the 0-0 transition of non-aggregated molecules. A possible explanation could be that the transition dipoles are not parallel in the aggregate which could lead to a splitting rather than a neat shift of the absorption band (88,89,90). For the film of polymer 1, there is no shift of the absorption peak. The spectrum is only slightly broadened compared to the solution which could be attributed to

an increased degree of disorder (61). While for polymer 1 a similar Stokes shift is observed in the film and in a solution of toluene it is for triad 1 about two times smaller in the film. This could be due to line narrowing induced by the exciton interaction (91). It should be noted that the absorption spectrum of the film of triad 1 shows a very broad tail on the red side which extends to 1000 nm, *i.e.*, 300 nm beyond the maximum of the fluorescence spectrum of this film. The origin of this tail is not clear. To get further information on the origin of this tail we recorded fluorescence excitation spectra of the emission at 700 nm and 800 nm of a film of triad 1 (See Data S4 Fig S4). Although these spectra show a pronounced shoulder in the range 610-615 nm, *i.e.* close to the maximum of the absorption spectrum of the film of triad 1, their onset is situated around 700 nm. This means that excitation in the long wavelength tail of the absorption spectrum does not lead to the generation of an emitting species. It is quite improbable that the tail can be attributed to trivial light scattering as in this case it should be even more pronounced at shorter wavelengths (light scattering is proportional to the inverse fourth power of the wavelength). As the long wavelength absorption band of triad 1 was characterized by a large molar extinction coefficient one cannot exclude the occurrence of refractive index changes and anomalous dispersion in the neighborhood of this band (92). This could lead to metallic specular reflection in this wavelength range reducing transmittance and thus yielding modified absorption spectra (when measured with a conventional spectrometer) stretched to longer wavelength regions. If this were the case, one would expect a similar change in the absorption spectrum of polymer 1, characterized by a similar molar extinction coefficient. The latter was however not observed. In case the tail is due to genuine light absorption it could be attributed to an intermolecular charge transfer absorption band (93) where an electron from an ICZ moiety of one molecule is transferred to a BODIPY moiety of a

neighboring molecule. Due to a different packing in the film of polymer 1 (suggested by a much smaller red shift of the absorption maximum compared to a dilute solution) such charge transfer state is probably less stabilized in a film of polymer 1 which could explain why this transition does not yield a long wavelength tail in the absorption spectrum of a film of polymer 1.

## CONCLUSIONS

We have reported here the synthesis and spectroscopic properties of a ICZ–π–BODIPY triad (triad 1) and corresponding alternating conjugated polymer (polymer 1). A red shift and an increase in band width of both absorption and emission spectra were observed for triad 1 and polymer 1 relative to their parent BODIPYs. This suggests a strong interaction between the BODIPY and ICZ chromophores. The major red shift of the emission upon increasing the solvent polarity as well as the decrease in fluorescence quantum yield of both compounds suggest an excited state with a significant dipole and therefore charge transfer character. The smaller Stokes shift and the less extensive solvent dependence of the emission maximum in polymer 1 compared to triad 1 suggest a smaller excited state dipole moment in polymer 1. The fluorescence decays and their solvent dependence suggest furthermore that this initial excited state is in equilibrium with a non-emitting state with enhanced charge separation. Upon excitation at 410 nm in the absorption band of ICZ, a very weak emission of the residual ICZ was observed, suggesting incomplete quenching and/or an ICZ impurity. Assuming incomplete quenching, the estimation of the quenching efficiency based on the fluorescence quantum yields, for both triad 1 and polymer 1 is 98 - 99 % in all three solvents used. The

similarity of the values of the fluorescence quantum yield of the long wavelength BODIPY centered emission, observed upon excitation either at 410 nm in the ICZ centered band or at 515 nm in the BODIPY centered band, indicates that the quenching is nearly exclusively due to energy transfer. The maximum values of the rate constants for energy transfer obtained from time-resolved fluorescence experiments are compatible with Förster type energy transfer calculated for a planar configuration, if the actual size of the chromophores is taken into account.

An alternating conjugated polymer, ICZ–π–DPP (polymer 2), was also synthesized where an excited state with partial charge transfer character was in equilibrium with a state with more extensive charge separation. However, compared to the ICZ–π–BODIPY compounds a much smaller red shift of both absorption and emission spectra was observed while the quenching efficiency amounted to only 82-88 %. This lower efficiency for energy transfer could, in the framework of Förster transfer, be attributed mainly to a decrease of the orientation factor $\kappa^2$. While for triad 1 and polymer 1, the broad distribution of decay times of the residual ICZ centered emission at 410 nm could still be attributed to the presence of impurities, this becomes highly unlikely for polymer 2 in view of the large fraction of molecules with long decay time. More likely would be that the rotation of the acceptor (DPP moiety) around the triple bond leads to a further decrease of $\kappa^2$ and the rate constant for energy transfer. Hence for polymer 2 the multi-exponential decay could reflect a distribution of orientations for rotation around the triple bond.

In contrast to the solution samples, a broader absorption spectrum with the maximum shifted nearly 100 nm (0.35 eV) to the longer wavelengths is observed for a spin-coated film of the

triad 1. This shift could suggest a packing of the molecules of triad 1 resembling a J-aggregate or a highly disordered H-aggregate (88,89,90). However, there is no shift of the absorption peak for the film of polymer 1 compared to dilute solution. The spectrum is only slightly broadened suggesting an increase of the environmental disorder in the solid state (61).

To improve the efficiency of organic solar cells an optimal coverage of the terrestrial solar emission spectrum is highly desired. This requires small molecules or conjugated polymers absorbing at longer wavelengths than those used currently. Both triad 1 and polymer 1 have a broad absorption spectrum that, especially in film, extends to longer wavelengths than the benchmark material P3HT (88,89,90). This will lead to a better coverage of the solar spectrum. Furthermore the charge transfer nature of the excited state can be advantageous for improved charge separation. Future work will be to study the behavior of bulk heterojunctions of triad 1 and polymer 1 with a suitable electron acceptor as PCBM and to make and characterize OPVs based on these combinations.

## **ACKNOWLEDGMENTS**:

The authors thank the Research Fund of the K.U. Leuven for financial support through GOA2011/3 and ZWAP 4/07 and the Belgium Science Policy through IAP 6/27 and 7/05. The authors thank the EU through the Marie Curie network “Herodot” (grant 214954) for a fellowship to AK. The authors are indebted to the IWT for a PhD grant to AC and MV.

## SUPPLEMENTARY MATERIALS

Additional Supporting Information may be found in the online version of this article.

**Data S1**: Fluorescence decays of the long wavelength emission of triad 1, polymer 1 and polymer 2 excited at 410 nm.

**Data S2:** Comparison of the excitation and absorption spectra of triad 1, polymer 1 and polymer 2.

**Data S3:** Transition dipole orientation in DPP 1.

**Data S4:** Excitation spectra of the films of triad 1 and polymer 1.

## REFERENCES


1. Perlin, J. (2004) The Silicon Solar cells turn 50, National Renewable Energy Laboratory, Report No. BR-520-33947.
2. Widenborg P.I., Aberle, A.G. (2007) Polycrystalline Silicon Thin-Film Solar Cells on AIT-Textured Glass Superstrates, Advance in Optoelectronics, vol. 2007, 24584.
3. Poortmans J., V. Arkhipov (2006) Thin Film Solar Cells; Fabrication, Characterization and Applications, pp 387-422. John Wiley & Sons Ltd, Chichester.
4. Dennler G., N.S. Sariciftci (2005) Flexible Conjugated Polymer-Based Plastic Solar Cells: From Basics to Applications. Proc. IEEE, 93, 1429-1439.
5. Li G., R. Zhu, Y. Yang (2012) Polymer solar cells. Nature Photonics, 6, 153-161.
6. Ma W.L., C.Y. Yang, X. Gong, K. Lee, A.J. Heeger (2005) Thermally Stable, Efficient Polymer Solar Cells with Nanoscale Control of the Interpenetrating Network Morphology. Adv. Funct. Mater. 15, 1617-1622.
7. Kim J.Y., K.H. Lee, N.E. Coates, D. Moses, T.Q. Nguyen, M. Dante, A.J. Heeger (2007) Efficient Tandem Polymer Solar Cells Fabricated by All-Solution Processing. Science, 317, 222-225.
8. Chen H.Y., J. Hou, S. Zhang, Y. Liang, G. Yang, Y. Yang, L. Yu, Y. Wu, G. Li (2009) Polymer solar cells with enhanced open-circuit voltage and efficiency. Nature Photonics, 3, 649-653.

9. Liang Y., Z. Xu, J. Xia, S.T. Tsai, Y. Wu, G. Li, C. Ray, L. Yu (2010) For the Bright Future-Bulk Heterojunction Polymer Solar Cells with Power Conversion Efficiency of 7.4%. Adv. Mater. 22, E135-E138.
10. Winder C., N.S. Sariciftci (2004) Low bandgap polymers for photon harvesting in bulk heterojunction solar cells. J. Mater. Chem. 14, 1077-1086.
11. Hou J., H.Y. Chen, S. Zhang, R. I. Chen, Y. Yang, Y. Wu, G. Li (2009) Synthesis of a Low Band Gap Polymer and Its Application in Highly Efficient Polymer Solar Cells. J. Am. Chem. Soc. 131, 15586-15587.
12. Blouin N., A. Michaud, M. Leclerc (2007) A Low-Bandgap Poly(2,7-Carbazole) Derivative for Use in High-Performance Solar Cells. Adv. Mater. 19, 2295-2300.
13. Mühlbacher D., M. Scharber, M. Morana, Z. Zhu, D. Waller, R. Gaudiana, C. Brabec (2006) High Photovoltaic Performance of a Low-Bandgap Polymer. Adv. Mater. 18, 2884-2889.
14. Zhang F., E. Perzon, X. Wang, W. Mammo, M.R. Andersson, O. Inganäs (2005) Polymer solar cells based on a low-bandgap fluorene copolymer and a fullerene derivative with photocurrent extended to 850 nm, Adv. Funct. Mater. 15, 745-750.
15. Peet J., J.Y. Kim, N.E. Coates, W.L. Ma, D. Moses, A.J. Heeger, G.C. Bazan (2007) Efficiency enhancement in low-bandgap polymer solar cells by processing with alkane dithiols. Nature Materials, 6, 497-500.
16. Nielsen C.B., R.S. Ashraf, B.C. Schroeder, P. D'Angelo, S.E. Watkins, K. Song, T. D. Anthopoulos, I. McCulloch (2012) Random benzotrithiophene-based donor-acceptor copolymers for efficient organic photovoltaic devices, Chem. Commun. 48, 5832-5834.
17. Ziessel R., C. Goze, G. Ulrich, M. Césario, P. Retailleau, A. Harriman, J.P. Rostron (2005) Intramolecular Energy Transfer in Pyrene–Bodipy Molecular Dyads and Triads. Chem. Eur. J. 11, 7366-7378.
18. Zrig S., P. Rémy, B. Andrioletti, E. Rose, I. Asselberghs, K. Clays (2008) Engineering tunable light-harvesting systems with oligothiophene donors and mono- or bis-bodipy acceptors. J. Org. Chem. 73, 1563-1566.

19. Suzukia S., M. Kozakia, K. Nozakib, K. Okada (2011) Recent progress in controlling photophysical processes of donor–acceptor arrays involving perylene diimides and boron-dipyrromethenes. J. Photochem. Photobiol. C: Photochem. Rev., 12, 269-292.
20. Hattori S., K. Ohkubo, Y. Urano, H. Sunahara, T. Nagano, Y. Wada, N.V. Tkachenko, H. Lemmetyinen, S. Fukuzumi (2005) Charge separation in a nonfluorescent donor-acceptor dyad derived from boron dipyrromethene dye, leading to photocurrent generation. J. Phys. Chem. B 109, 15368-15375.
21. Balan A., D. Baran, L. Toppare (2011) Benzotriazole containing conjugated polymers for multipurpose organic electronic applications. Polym. Chem. 2, 1029-1043.
22. Marrocchi A., F. Silvestri, M. Seri, A. Facchetti, A. Taticchi, T.J. Marks (2009) Conjugated anthracene derivatives as donor materials for bulk heterojunction solar cells: olefinic versus acetylenic spacers. Chem.Commun. 45, 1380-1382.
23. Silvestri F., A. Marrocchi (2010) Acetylene-Based Materials in Organic Photovoltaics, Int. J. Mol. Sci. 11, 1471-1508
24. Guldi D. M. (2010) Putting a positive spin on molecular bridges. Angew. Chem. Int. Ed. 49, 7844-7846.
25. Wu Y., Y. Li, S. Gardner, B. S. Ong (2005) Indolo[3,2-*b*]carbazole-Based Thin-Film Transistors with High Mobility and Stability. J. Am. Chem. Soc. 127, 614-618.
26. Li Y., Y. Wu, B. S. Ong (2006) Polyindolo[3,2-*b*]carbazoles: A New Class of p-Channel Semiconductor Polymers for Organic Thin-Film Transistors**.** Macromolecules, 39, 6521-6527.
27. Boudreault P.-L. T., S. Wakim, N. Blouin, M. Simard, C. Tessier, Y. Tao, M. Leclerc (2007) Synthesis, characterization, and application of indolo[3,2-b]carbazole semiconductors. J. Am. Chem. Soc. 129, 9125-9136.
28. Guo Y., H. Zhao, G. Yu, C.-a. Di, W. Liu, S. Jiang, S. Yan, C. Wang, H. Zhang, X. Sun, X. Tao, Y. Liu (2008) Single-Crystal Microribbons of an Indolo[3,2-*b*]carbazole Derivative by Solution-Phase Self-Assembly with Novel Mechanical, Electrical, and Optical Properties. Adv. Mater. 20, 4835-4839.

29. Boudreault P.-L.T., A.A. Virkar, Z. Bao, M. Leclerc (2010) Synthesis and characterization of soluble indolo[3,2-*b*]carbazole derivatives for organic field-effect transistors. Org. Electron. 11, 1649-1659.
30. Zhao H.-P., X.-T. Tao, P. Wang, Y. Ren, J.-X. Yang, Y.-X. Yan, C.-X. Yuan, H.-J. Liu, D.-C. Zou, M.-H. Jiang (2007) Effect of substituents on the properties of indolo[3,2 *b*]carbazole-based hole-transporting materials. Org. Electron. 8, 673-682.
31. Zhao H.-P., X.-T. Tao, F.-Z. Wang, Y. Ren, X.-Q. Sun, J.-X. Yang, Y.-X. Yan, D.-C. Zou, X. Zhao, M.-H. Jiang (2007) Structure and electronic properties of triphenylamine-substituted indolo[3,2-*b*]carbazole derivatives as hole-transporting materials for organic light-emitting diodes. Chem. Phys. Lett. 439, 132-137.
32. Zhao H.-P., F.-Z. Wang, C.-X. Yuan, X.-T. Tao, J.-L. Sun, D.-C. Zou, M.-H. Jiang (2009) Indolo[3,2-*b*]carbazole: Promising building block for highly efficient electroluminescent materials**.** Org. Electron. 10, 925-931.
33. Lengvinaite S., J. V. Grazulevicius, S. Grigalevicius, R. Gu, W. Dehaen, V. Jankauskas, B. Zhang, Z. Xie (2010) Indolo[3,2-*b*]carbazole-based functional derivatives as materials for light emitting diodes. Dyes Pigm. 85, 183-188.
34. Zhou E., S. Yamakawa, Y. Zhang, K. Tajima, C. Yang, K. Hashimoto (2009) Indolo[3,2-*b*]carbazole-based alternating donor–acceptor copolymers: synthesis, properties and photovoltaic application. J. Mater. Chem. 19, 7730-7737.
35. Xia Y., X. Su, Z. He, X. Ren, H.Wu, Y. Cao, D. Fan (2010) An Alternating Copolymer Derived from Indolo[3,2-*b*]carbazole and 4,7-Di(thieno[3,2-*b*]thien-2-yl)-2,1,3-benzothiadiazole for Photovoltaic Cells. Macromol. Rapid Commun. 31, 1287-1292.
36. Zhou E., J. Cong, K. Tajima, K. Hashimoto (2010) Synthesis and Photovoltaic Properties of Donor−Acceptor Copolymers Based on 5,8-Dithien-2-yl-2,3-diphenylquinoxaline. Chem. Mater. 22, 4890-4895.
37. Zhang X.-H., Z.-S. Wang, Y. Cui, N. Koumura, A. Furube, K. Hara (2009) Organic Sensitizers Based on Hexylthiophene-Functionalized Indolo[3,2-*b*]carbazole for Efficient Dye-Sensitized Solar Cells. J. Phys. Chem. C 113, 13409-13415.
38. Van Snick S., W. Dehaen (2012) Synthesis of novel 2,8-disubstituted indolo[3,2-*b*]carbazoles. Org. Biomol. Chem. 10, 79-82.

39. Van der Auweraer M., J.C. Dederen, C. Palamans-Windels, F.C. De Schryver (1982) Fluorescence quenching by neutral quenchers in SDS-micelles. J. Am. Chem. Soc. 104, 1800-1804.
40. Qin W., V. Leen, T. Rohand, W. Dehaen, P. Dedecker, M. Van der Auweraer, K. Robeyns, L. Van Meervelt, D. Beljonne, B. Van Averbeke, J.N. Clifford, K. Driesen, K. Binnemans, N. Boens (2009) Synthesis, Spectroscopy, Crystal Structure, Electrochemistry, and Quantum Chemical and Molecular Dynamics Calculations of a 3-Anilino Difluoroboron Dipyrromethene Dye. J. Phys. Chem. A 113, 439-447.
41. Ulrich G., R.J. Ziessel (2004) Convenient and Efficient Synthesis of Functionalized Oligopyridine Ligands Bearing Accessory Pyrromethene-BF2 Fluorophores. Org. Chem. 69, 2070-2083.
42. Goud T.V., A. Tutar, J.F. Biellmann (2006) Synthesis of 8-heteroatom-substituted 4,4-difluoro-4-bora-3a,4a-diaza-*s*-indacene dyes (BODIPY). Tetrahedron, 62, 5084-5091.
43. Qin W., M. Baruah, M. Van der Auweraer, F.C. De Schryver, N. Boens (2005) Photophysical Properties of Borondipyrromethene Analogues in Solution. J. Phys. Chem. A, 109, 7371-7384.
44. Qin W., M. Baruah, A. Stefan, M. Van der Auweraer, N. Boens (2005) Photophysical properties of BODIPY-derived hydroxyaryl fluorescent pH probes in solution. ChemPhysChem. 6, 2343-2351.
45. Baruah M., W. Qin, R. A. L. Valle´e, D. Beljonne, T. Rohand, W. Dehaen, N. Boens (2005) A Highly Potassium-Selective Ratiometric Fluorescent Indicator Based on BODIPY Azacrown Ether Excitable with Visible Light. Org. Lett. 7, 4377-4380.
46. Rohand T., M. Baruah, W. Qin, N. Boens, W. Dehaen (2006) Functionalisation of fluorescent BODIPY dyes by nucleophilic substitution. Chem. Commun. 42, 266–268.
47. Qin W., T. Rohand, W. Dehaen, J. N. Clifford, K. Driessen, D. Beljonne, B. Van Averbeke, M. Van der Auweraer, N. Boens (2007) Boron dipyrromethene analogs with phenyl, styryl, and ethynylphenyl substituents: synthesis, photophysics, electrochemistry, and quantum-chemical calculations. J. Phys. Chem. A, 111, 8588-8597.

48. Tieke B., A.R. Rabindranath, K. Zhang, Y. Zhu, (2010) Conjugated polymers containing diketopyrrolopyrrole units in the main chain. Beilstein J. Org. Chem. 6, 830-845.
49. Kim Y., C. Eun Song, A. Cho, J. Kim, Y. Eom, J. Ahn, S.-J. Moon, E. Lim (2014) Synthesis of diketopyrrolopyrrole (DPP)-based small molecule donors containing thiophene or furan for photovoltaic applications. Mat. Chem. Phys. 143, 825-829.
50. Kirkus M., L. Wang, S. Mothy, D. Beljonne, J. Cornil, R.A.J. Janssen, S.C.J. Meskers (2012) Optical properties of Oligothiophene Substituted Diketopyrrolopyrrole Derivatives in the Solid phase: Joint J- and H-Type Aggregation. J. Phys. Chem. A 116, 7927-7936.
51. Li W., A. Furlan, K.H. Hendriks, M.M. Wienk, R.A.J. Janssen (2013) Efficient Tandem and Triple-Junction Polymer Solar Cells. J. AM. Chem. Soc., 135, 5529-5532.
52. Palai A.K, J. Lee, M. Jea, H. Na, T. Joo Shin, S. Jang, S.-U. Park, S. Po (2014) Symmetrically functionalized diketopyrrolopyrrole with alkylated thiophene moiety: from synthesis to electronic devices applications. J. Mater. Sci., 49, 4215-4222.
53. Leen V., E. Braeken, K. Luckermans, C. Jackers, M. Van der Auweraer, N. Boens, W. Dehaen (2009) A versatile, modular synthesis of monofunctionalized BODIPY dyes. Chem. Commun. 45, 4515-4517.
54. Iqbal A., M. Jost, R. Kirchmayr, J. Pfenninger, A. Rochat, O. Walquist (1988) The synthesis and properties of 1,4-diketo-pyrrolo[3,4-C]pyrroles. Bull Soc. Chim. Belg., 97, 615-644.
55. Maus M., E. Rousseau, M. Cotlet, G. Schweitzer, J. Hofkens, M. Van der Auweraer, F.C. De Schryver, A. Krueger (2001) New picosecond laser system for easy tunability over the whole ultraviolet/visible/near infrared wavelength range based on flexible harmonic generation and optical parametric oscillation. Rev. Sci. Instrum., 72, 36-40.
56. Filarowski A., M. Kluba, K. Cieslik-Boczula, A. Koll, A. Kochel, L. Pandey, W.M. De Borggraeve, M. Van der Auweraer, J. Catalan, N. Boens (2010) Generalized solvent scales as a tool for investigating solvent dependence of spectroscopic and kinetic parameters. Application to fluorescent BODIPY dyes. Photochem. Photobiol. Sci. 9, 996-1008.

57. Thomsson D., R. Camaho, Y. Tina, D. Yadav, G. Sforazzzini, H.L. Anderson, I.G. Scheblykin (2009) Cyclodextrin Insulation Prevents Static Quenching of Conjugated Polymer Fluorescence at the Single Molecule Level. Small, 15, 2619-2627.
58. Lin H., Y. Tian, K. Zapadka, G. Persson, D. Thomsson, O. Mirzov, P.-O. Larsson, J. Widengren, I.G. Scheblykin (2009) Fate of Excitations in Conjugated Polymers: Single-Molecule Spectroscopy Reveals Nonemissive: "Dark" Regions in MEH-PPV Individual Chains. Nanoletters, 8, 4456-4461.
59. Mizuguchi J., T. Imoda, H. Takahashi, H. Yamakami (2006) Polymorph of 1,4-diketo-3,6-bis-(4′-dipyridyl)-pyrrolo-[3,4-*c*]pyrrole and their hydrogen bond network: A material for $H_2$ gas sensor. Dyes Pigm. 68, 47-52.
60. Verheijen W., J. Hofkens, B. Mertens, J. Vercammen, R. Shukla, M. Smet, W. Dehaen, Y. Engelborghs, F. De Schryver (2005) The Photo Physical Properties of Dendrimers Containing 1,4-Dioxo-3,6-Diphenylpyrrolo[3,4-c]pyrrole (DPP) as a core, Marcromol. Chem. Phys. 206, 25-32.
61. Bässler H. (1981) Localized states and electronic transport in single component organic solids with diagonal disorder. Phys. Stat. Sol. b, 107, 9-54.
62. Wui M.H., W.R. Ware (1976) Exciplex Photophysics. III. Kinetics of fluorescence quenching of a-cyanonaphthalene by dimethylcyclopentene-1,2 in hexane. J. Am Chem. Soc. 98, 4706-4711.
63. Wui M.H., W.R. Ware (1976) The kinetics of fluorescence quenching of anthracene by N,N-dimethylaniline in cyclohexane. J. Am Chem. Soc. 98, 4718-4727.
64. O'Connor D.V., W.R. Ware (1979) Exciplex Photophysics. 6. Quenching of a-cyanonaphthalene by dimethylcyclopentene-1,2 in slightly polar solvents. J. Am. Chem. Soc. 101, 121-128.
65. Fron E., M. Lor, R. Pilot, G. Schweitzer, H. Dincalp, S. De Feyter, J. Cremer, P. Bäuerle, K. Müllen, M. Van der Auweraer, F.C. De Schryver (2005) Photophysical Study of Photoinduced Electron Transfer in a Bis-thiophene Substituted Peryleneimide. Photochem. Photobiol. Sci. 5, 61-68.
66. Fron E., T. Bell, A. Van Vooren, G. Schweitzer, J. Cornil, D. Beljonne, P. Toele, J. Jacob, K. Müllen, J. Hofkens, M. Van der Auweraer, F. C. De Schryver (2007) CT-CT

Annihilation in Rigid Perylene End-Capped Pentaphenylenes. J. Am. Chem. Soc. 129, 610-619.

67. Van der Auweraer M., Z. Grabowski, W. Rettig (1991) Molecular Structure and the temperature dependent, radiative rates in TICT and exciplex systems. J. Phys. Chem. 95, 2083-2092.
68. Verhoeven J.W., M.N. Paddon-Row, J.M. Warman (1992) Photoprocesses in Transition Metal Complexes, Biosystems and Other Molecules. Experiment and Theory (Eds. E. Kocharski) NATO ASI Series C, 376, 271-298 Kluwer Academic, Dordrecht (The Netherlands). (ISBN 978-94-010-5195-8)
69. Siders P., R. A. Marcus (1981) Quantum effects in electron-transfer reactions, J. Am. Chem. Soc. 103, 741-747.
70. Siders P., R. A. Marcus (1981) Quantum effects for electron-transfer reactions in the "inverted region". J. Am. Chem. Soc. 103, 748-752.
71. Marcus R.A. (1984) Nonadiabatic processes involving quantum-like and classical-like coordinates with applications to nonadiabatic electron transfers. J. Chem. Phys. 81, 4494-4500.
72. Hungerford G., Van der Auweraer M., Chambron J.-C., Heitz V., Sauvage J.-P., Pierre J.-L., Zurita D. (1999) Intramolecular Energy Transfer in Bis-porphyrins Containing Diimine Chelates of Variable Geometry as Spacers. Chem. Eur. J. 5, 2089-2100.
73. Reeta P.S., Khetubol A., Jella T., Chukharev V., Abou-Chahine F., Tkachenko N.V., Giribabu L., Lemmetyinen H. (2015) Photophysical properties of Sn(IV)tetraphenylporphyrin-pyrene dyad with a β–vinyl linker. J. Porphyrins Phthalocyanines 19, in press (JPP 140251).
74. Förster T. (1951) Fluorezenz Organische Verbindungen, Göttingen: Vandenhoeck and Ruprecht.
75. Förster T. (1959) Transfer Mechanisms of Electronic Excitation. Disc. Far. Soc. 27, 7-17.
76. Agranovich V.M., M.D. Galanin (1982) Electronic Excitation Energy Transfer in Condensed Matter, Modern Problems in Condensed Matter Science 3; North Holland Publishing Company, Amsterdam.

77. Czikklely V., H.D. Forsterling, H. Kuhn (1970) Extended dipole model for aggregates of dye molecules. Chem. Phys. Lett. 6, 207-210.
78. Czikklely V., H.D. Forsterling, H. Kuhn (1970) Light absorption and structure of aggregates of dye molecules. Chem. Phys. Lett. 6, 11-14.
79. Norland K., A. Ames, T. Taylor (1970) Spectral shifts of aggregated sensitizing dyes. Photogr. Sci. Eng. 14, 295-307.
80. Chang J.C. (1977) Monopole effects on electronic excitation interactions between large molecules: Application to energy transfer in chlorophylls. J. Chem. Phys. 67, 3901-3909.
81. Krueger B.P., G.D. Scholes, G.R. Fleming (1998) Calculation of Couplings and Energy-Transfer Pathways between the Pigments of LH2 by the ab INITIO Transition Density Cube Method. J. Phys. Chem B 102, 5378-5386.
82. Scholes G.D., K.P. Ghiggino (1994) Electronic Interactions and Interchromophore Excitation Transfer. J. Phys. Chem. 98, 4580-4590.
83. Scholes G.D. (1996) Energy Transfer and Spectroscopic Characterization of Multichromophoric Assemblies. J. Phys. Chem. 100, 18731-39.
84. Harcourt R.D., G.D. Scholes, K.P. Ghiggino (1994) Rate expressions for excitation transfer: II Electronic considerations. J. Chem. Phys. 101, 10521-5.
85. Dexter D. L. (1953) A theory of sensitized luminescence in solids. J. Chem. Phys. 21, 836-850.
86. Clayton A.H.A., G.D. Scholes, K.P. Ghiggino, M.N. Paddon-Row (1996) Through-Bond and Through-Space Coupling in Photoinduced Electron and Energy Transfer: An *ab Initio* and Semiempirical Study. J. Phys. Chem. 100, 10912-8.
87. Curutchet C., B. Mennucci, G.D. Scholes, D. Beljonne (2008) Does Förster Theory predict the Rate of Electronic Energy Transfer for a Model Dyad at Low temperature. J. Phys. Chem. B 112, 3759-3766.
88. Spano F.C. (2005) Modeling disorder in polymer aggregates: The optical spectroscopy of regioregular poly(3-hexylthiophene) thin films. J. Chem. Phys. 122, 234701.
89. Spano F.C. (2006) Absorption in regio-regular poly(3-hexyl)thiophene thin films: Fermi resonances, interband coupling and disorder. Chem. Phys. 325, 22-35.

90. Spano F.C., J. Clark, C. Silva, R.H. Friend (2009) Determining exciton coherence from the photoluminescence spectral line shape in poly(3-hexylthiophene) thin films. J. Chem. Phys. 130, 074904.
91. Chernyak V., T. Meier, E. Tsiper, S. Mukamel (1999) Scaling of Fluorescence Stokes Shift and Superradiance in Disordered Molecular Aggregates. J. Phys. Chem. A 103, 10294-10299.
92. Kittel C. (2005) Introduction to Solid State Physics Hoboken N.J.: John Wiley & Sons, p. 427-450.
93. Vandewal K., Gadisa A., Oosterbaan W.D., Bertho S., Banishoeib F., Van Severen I., Lutsen L., Cleij T.J., Vanderzande D., Manca, J.V. (2008) The Relation Between Open-Circuit Voltage and the Onset of Photocurrent Generation by Charge-Transfer Absorption in Polymer : Fullerene Bulk Heterojunction Solar Cells. Adv. Func. Mat. 18, 2064-2070.

## Figures and schemes

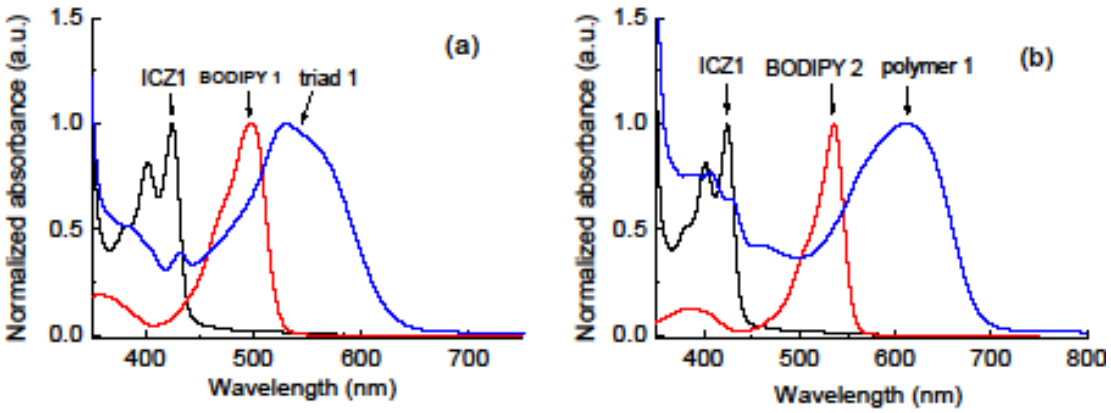


**Figure 1.** Absorption spectra normalized at the maximum of a solution of (a) ICZ 1, BODIPY 1 and triad 1; (b) ICZ 1, BODIPY 2 and polymer 1 in chloroform.

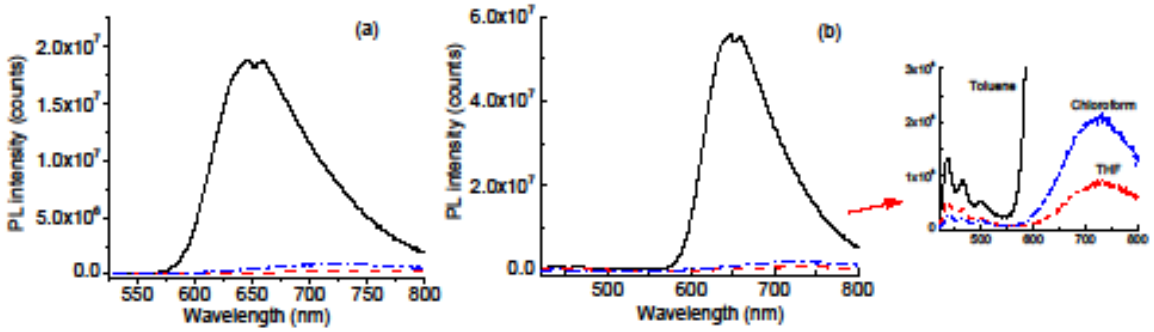


**Figure 2.** PL spectra of a solution of triad 1 in toluene (——), THF (– – –), and chloroform (– . – .). The excitation occurred at (a) 515 nm and (b) 410 nm.

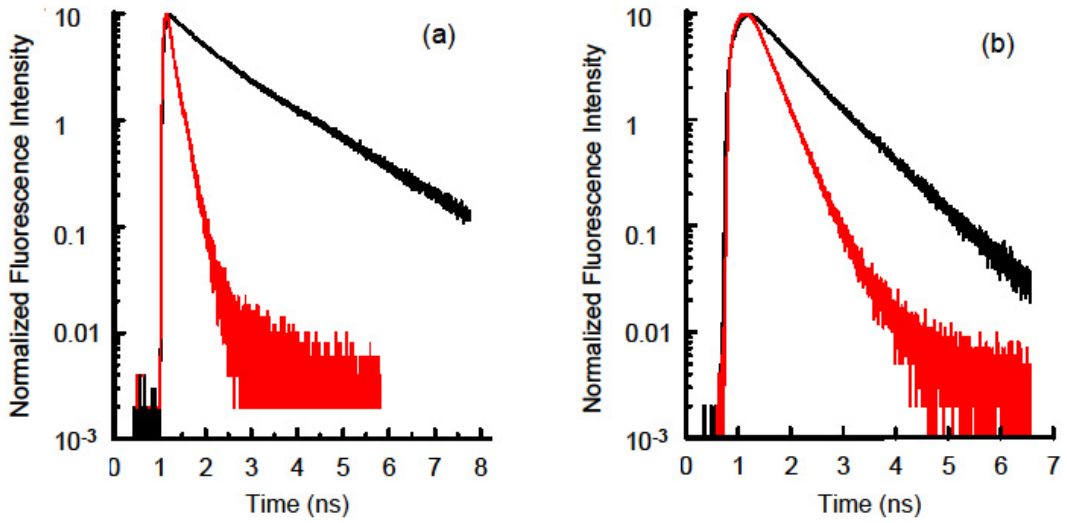


**Figure 3.** Normalized fluorescence decays of (a) triad 1 and (b) polymer 1, in toluene at 650 nm (triad 1) and 670 nm (polymer1), and in THF at 720 nm. The excitation occurred at 550 nm and 635 nm for respectively triad 1 and polymer 1.

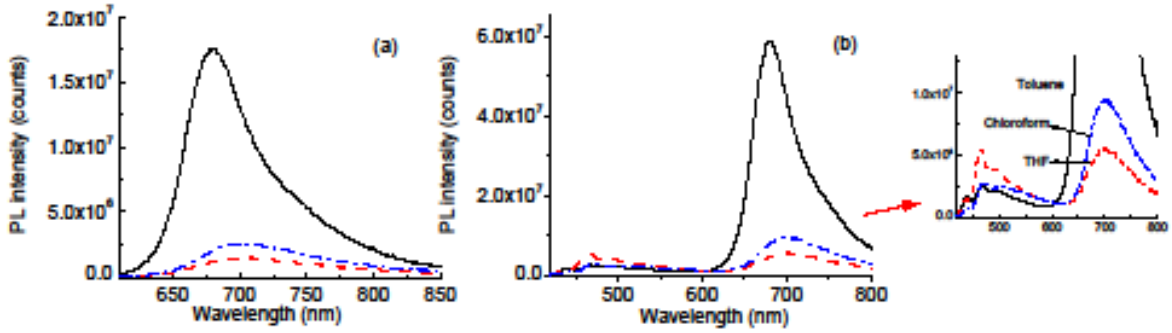


**Figure 4.** PL spectra of a solution of polymer 1 in toluene, THF (– – –), and chloroform (– · – · –). The excitation occurred at (a) 600 nm and (b) 410 nm.

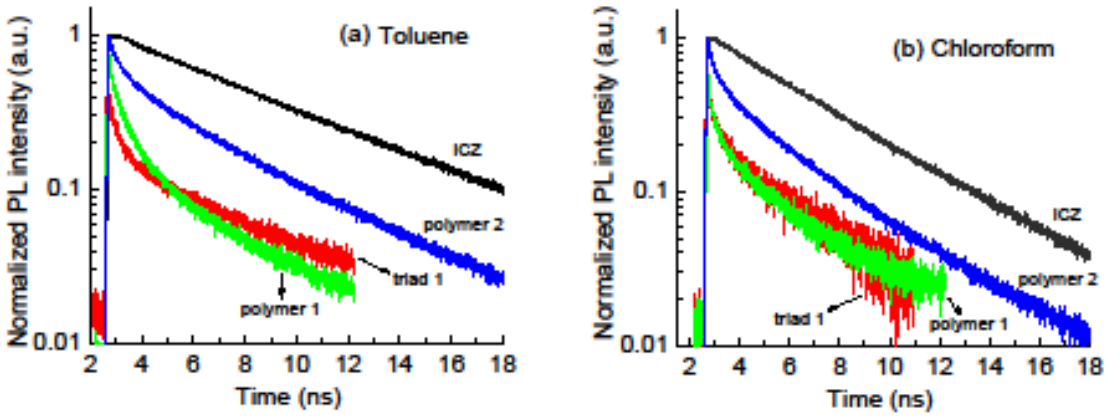


**Figure 5.** Normalized fluorescence decays of a solution of ICZ 1, triad 1, polymer 1, and polymer 2 in toluene (a) and chloroform (b), recorded at the emission wavelength ($\lambda_{em}$ ) of 460 nm, *i.e.* in the ICZ emission band. The excitation occurred at 410 nm.

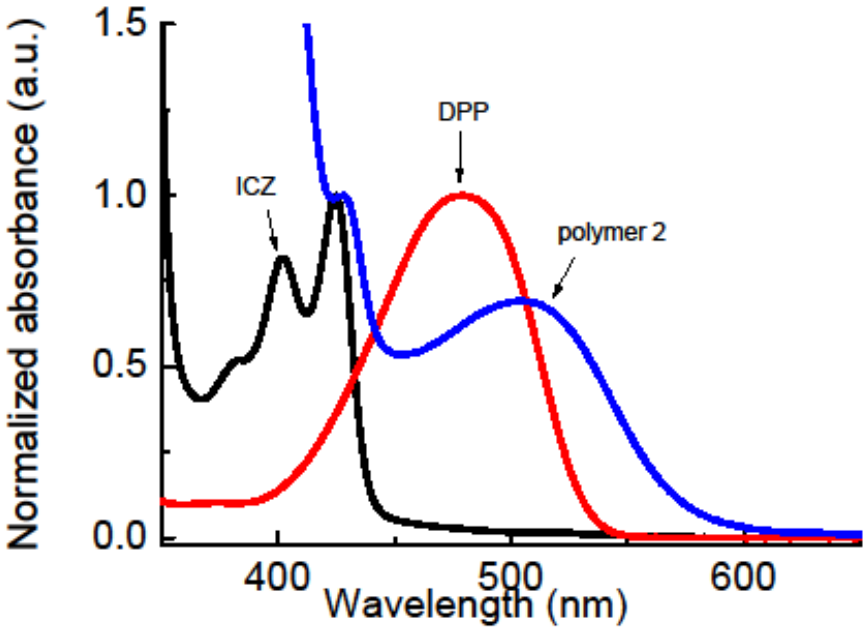


**Figure 6.** Absorption spectra normalized at the most intense maximum of a solution of ICZ 1, DPP 1, and polymer 2 in chloroform.

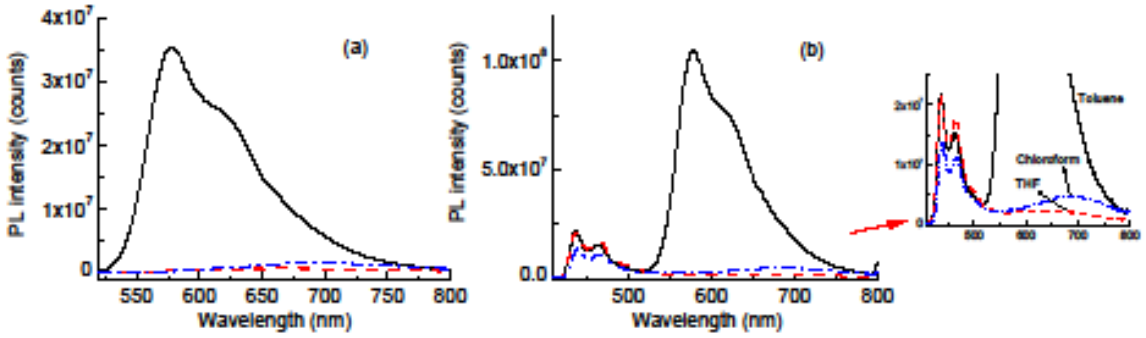


**Figure 7.** PL spectra of a solution of polymer 2 in toluene (——), THF (– – –), and chloroform (– · – · –). The excitation occurred at 515 nm (a) and 410 nm (b).

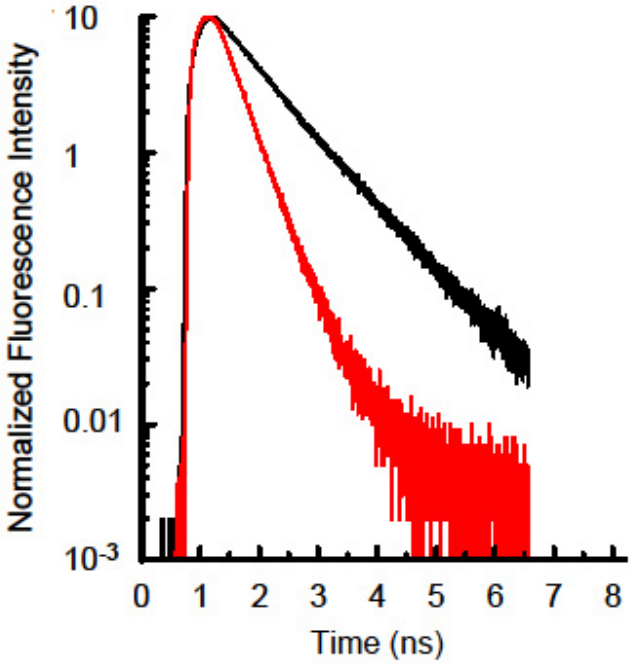


**Figure 8.** Normalized fluorescence decays of polymer 1 in toluene at 600 nm and in THF at 700 nm. The excitation occurred at 488 nm.

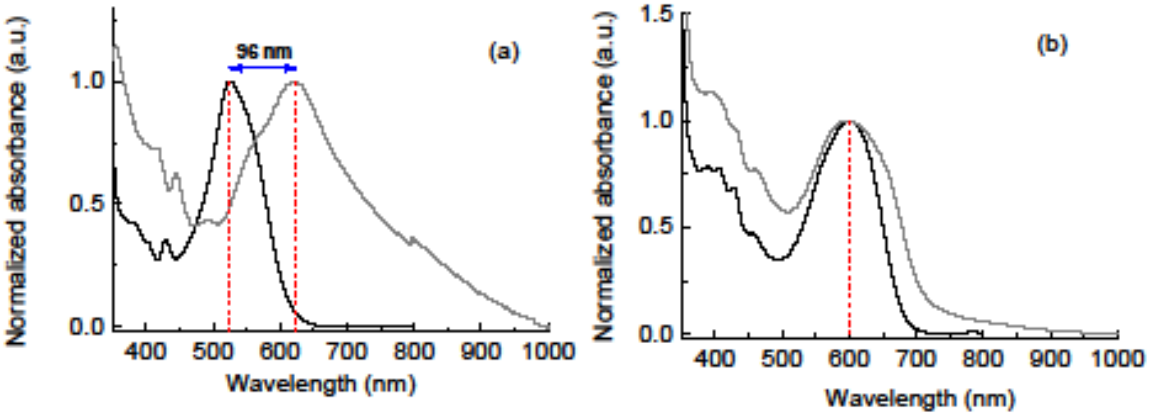


**Figure 9.** Normalized absorption spectra of a solution in toluene (black) and a spin-coated film (grey) of (a) triad 1 and (b) polymer 1.

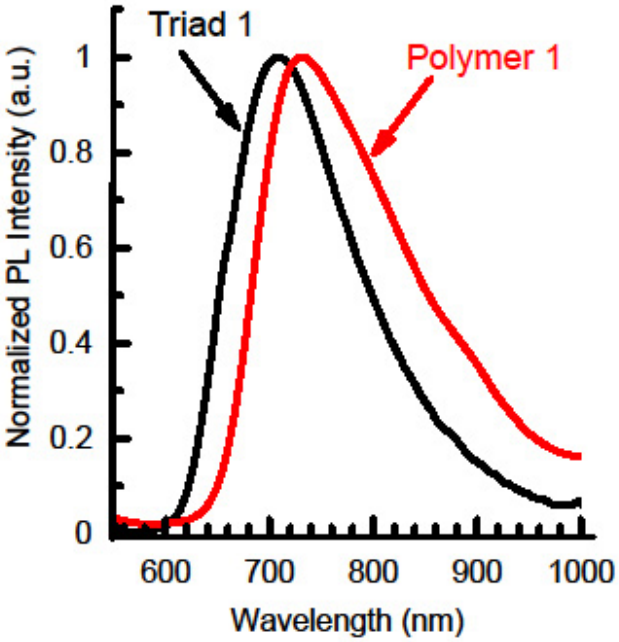


**Figure 10.** Normalized photoluminescence spectra of a spin-coated film of triad 1 and polymer 1. The excitation occurred at 515 nm.

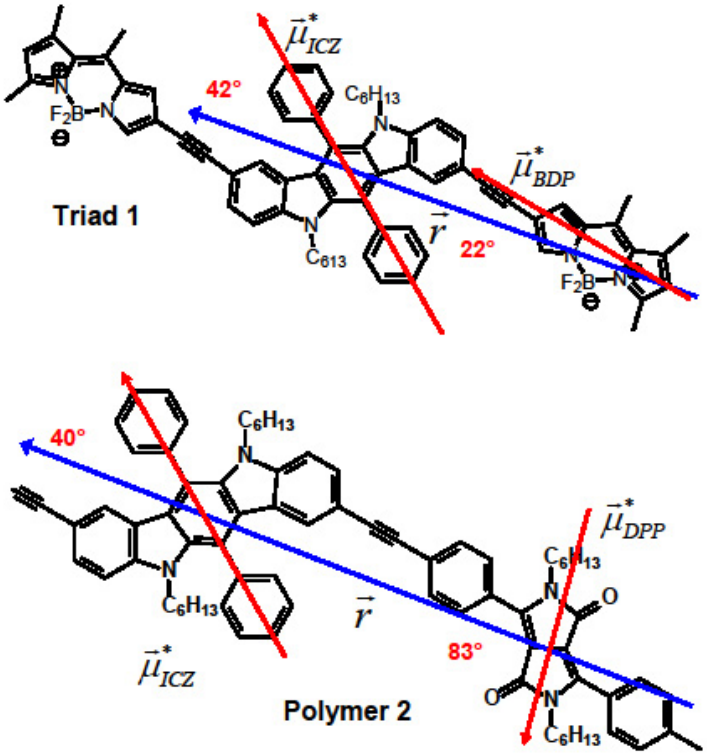


**Figure 11.** Orientation of the transition dipoles of the donor and acceptor centered transitions in the triad 1 or polymer 1 and polymer 2.

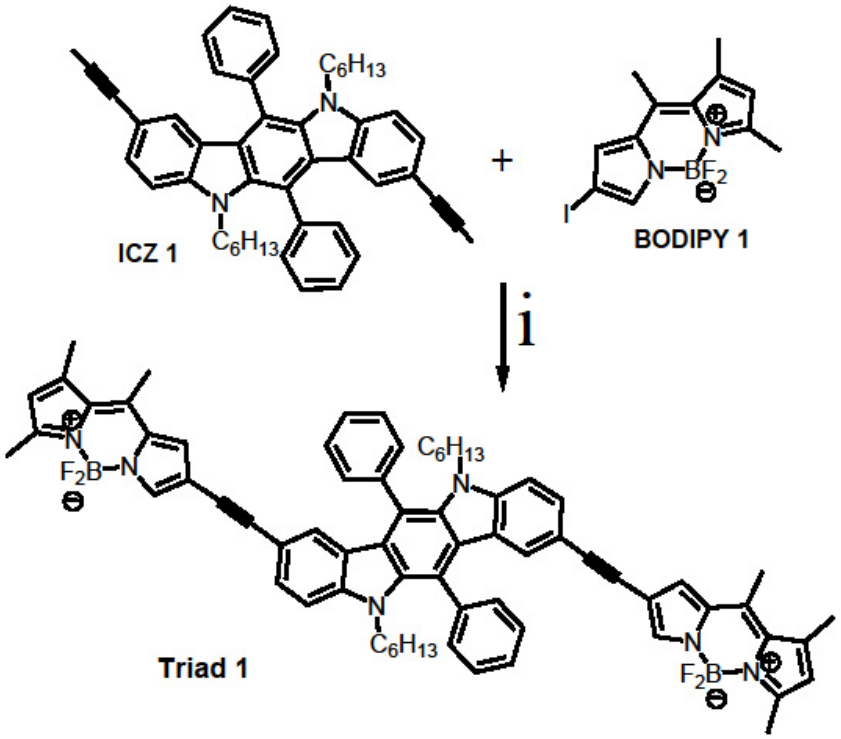


**Scheme 1.** Synthesis of the ICZ–π–BODIPY triad.

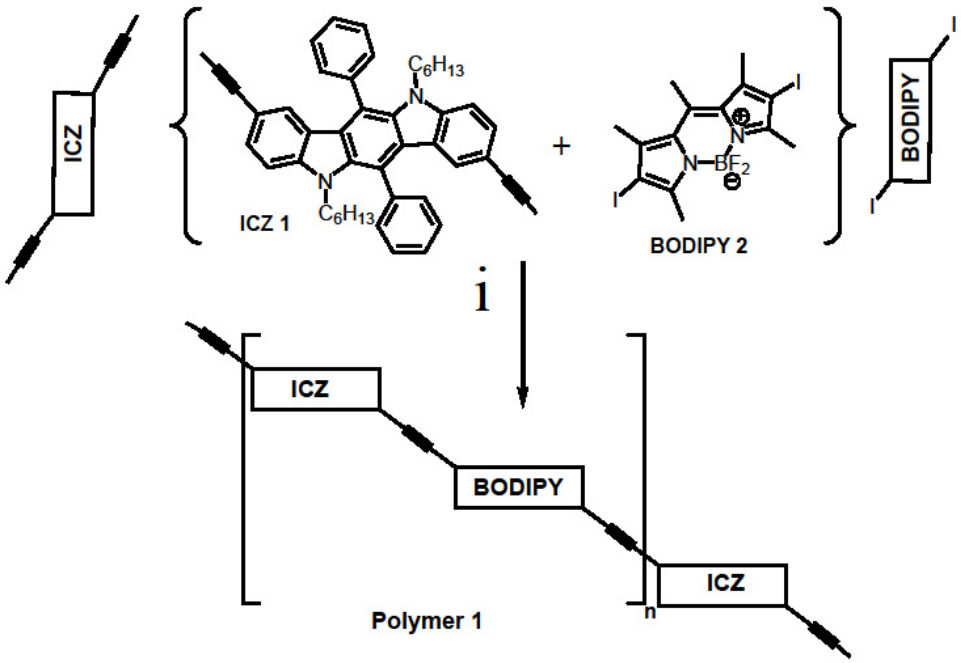


**Scheme 2.** Synthesis of the ICZ–π–BODIPY polymer (polymer1).

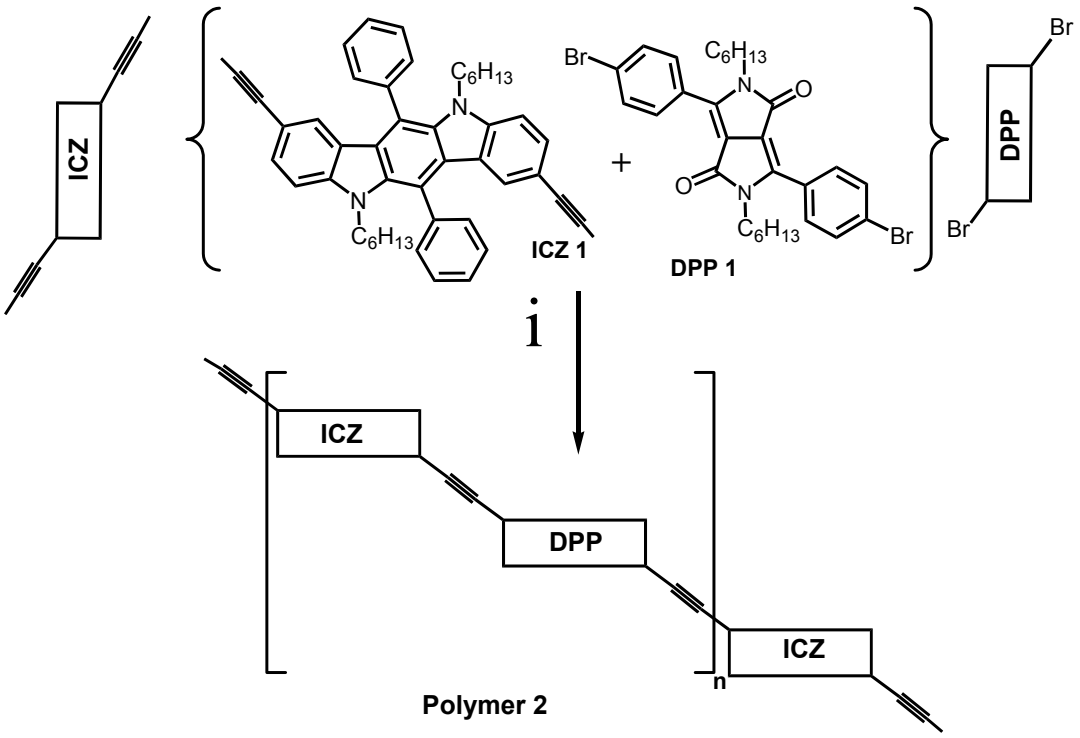


**Scheme 3.** Synthesis of the ICZ–π–DPP polymer (polymer2).

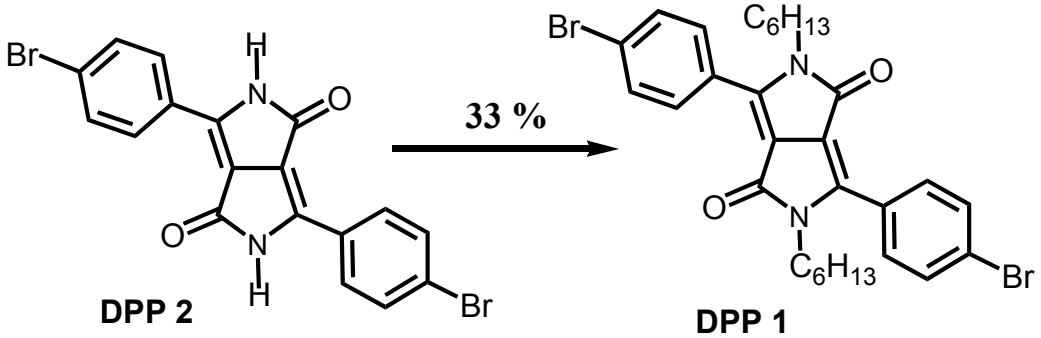


**Scheme 4.** Synthesis of DPP 1

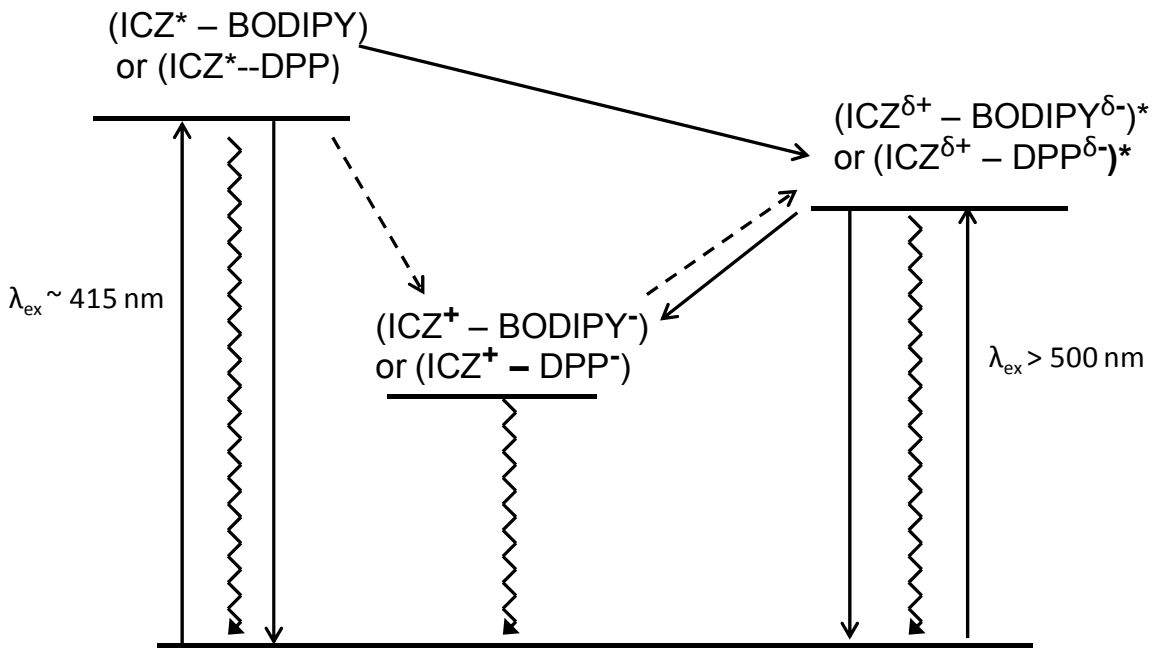


**Scheme 5**: Excited state kinetics of ICZ-BODIPY and ICZ-DPP conjugates

**Table 1.** Fluorescence decay amplitudes, decay times, amplitude-weighted average fluorescence decay times (Eq. 1) and fluorescent rate constant corresponding to the fluorescence intensity decays of the BODIPY centered emission of triad 1 obtained in toluene (TL), chloroform (CF) and THF. Excitation occurred at 550 nm.

| | | $A_1$ | $\tau_1$ | $A_2$ | $\tau_2$ | $\langle\tau\rangle$ | $\langle k_f \rangle$ |
|---|---|---|---|---|---|---|---|
| TL | 650 nm | 0.444 | 481 ps | 0.556 | 1.64 ns | 1.17 ns | $6.9 \times 10^7$ $s^{-1}$ |
| | 720 nm | 0.404 | | 0.596 | | | |
| CF | 650 nm | 0.975 | 256 ps | 0.025 | 1.508 ns | 273 ps | $1.8 \times 10^7$ $s^{-1}$ |
| | 720 nm | 0.968 | | 0.014 | | | |
| THF | 650 nm | 0.957 | 132 ps | 0.043 | 350 ps | 135 ps | $1.5 \times 10^7$ $s^{-1}$ |
| | 720 nm | 0.986 | | 0.014 | | | |

**Table 2.** Fluorescence decay amplitudes, decay times, amplitude-weighted average fluorescence decay times (Eq. 1) and fluorescence rate constant corresponding to the fluorescence intensity decays of the BODIPY centered emission of polymer 1 obtained in toluene (TL), chloroform (CF) and THF. Excitation occurred at 635 nm (TL and THF) or 644 nm (CF).

| | | $A_1$ | $\tau_1$ | $A_2$ | $\tau_2$ | $\langle\tau\rangle$ | $\langle k_f \rangle$ |
|---|---|---|---|---|---|---|---|
| TL | 670 nm | 0.378 | 506 ps | 0.622 | 904 ps | 772 ps | $7.1 \times 10^7$ $s^{-1}$ |
| | 720 nm | 0.388 | | 0.612 | | | |
| CF | 670 nm | 0.973 | 327 ps | 0.027 | 921 ns | 333 ps | $3.6 \times 10^7$ $s^{-1}$ |
| | 720 nm | 0.990 | | 0.010 | | | |
| THF | 670 nm | 0.978 | 228 ps | 0.022 | 730 ps | 234 ps | $2.1 \times 10^7$ $s^{-1}$ |
| | 720 nm | 0.989 | | 0.011 | | | |

**Table 3.** Fluorescence decay amplitudes ($A_i$), fluorescence decay times ($\tau_i$), amplitude-weighted average fluorescence decay times ($<\tau>$) as determined by Eq. 2, quenching efficiencies ($\Phi_{q\tau}$ as determined by Eq. 5 and average quenching rate constants ($<k_{q\tau}>$) as determined by Eq. 6, corresponding to the fluorescence intensity decays of the ICZ emission in Fig. 5 obtained in toluene and chloroform. Excitation occurred at 410 nm and the emission was recorded at 460 nm.

| | | $\tau_1$ (ns) | $A_1$ (%) | $\tau_2$ (ns) | $A_2$ (%) | $\tau_3$ (ns) | $A_3$ (%) | $<\tau>$ (ns) | $\Phi_{q\tau}$ (%) | $<k_{q\tau}>^a$ ($ns^{-1}$) |
|---|---|---|---|---|---|---|---|---|---|---|
| Toluene | ICZ 1 | 2.31 | 8 | 6.60 | 92 | | | 6.25 | | |
| | Triad 1 | $2.4x10^{-2}$ | 81 | 0.39 | 11 | 4.47 | 8 | 0.42 | 93.7 | 2.2 |
| | Polymer 1 | $7.4x10^{-2}$ | 50 | 0.65 | 37 | 3.99 | 13 | 0.81 | 87.1 | 1.1 |
| | Polymer 2 | 0.27 | 36 | 1.59 | 24 | 5.29 | 40 | 2.61 | 58.3 | 0.22 |
| Chloroform | ICZ 1 | 2.08 | 12 | 4.70 | 88 | | | 4.39 | | |
| | Triad 1 | $3.5x10^{-2}$ | 73 | 0.44 | 15 | 3.69 | 12 | 0.55 | 87.5 | 1.6 |
| | Polymer 1 | $1.9x10^{-2}$ | 85 | 0.28 | 9 | 2.56 | 6 | 0.20 | 95.4 | 4.8 |
| | Polymer 2 | 0.21 | 42 | 1.29 | 23 | 4.05 | 35 | 1.80 | 59 | 0.33 |

**Table 4.** Fluorescence decay amplitudes, decay times, amplitude-weighted average fluorescence decay times (Eq. 1) and fluorescence rate constant corresponding to the fluorescence intensity decays of the DPP centered emission of polymer 2 obtained in toluene (TL), chloroform (CF) and THF. Excitation occurred at 488 nm.

| | | $A_1$ | $\tau_1$ | $A_2$ | $\tau_2$ | $A_3$ | $\tau_3$ | $\langle\tau\rangle$ | $\langle k_f \rangle$ |
|---|---|---|---|---|---|---|---|---|---|
| TL | 600 nm | 0.331 | 1.22 ns | 0.669 | 3.01 ns | | | 2.42 ns | $2.7 \times 10^8$ $s^{-1}$ |
| | 650 nm | 0.322 | | 0.677 | | | | | |
| | 700 nm | 0.318 | | 0.682 | | | | | |
| CF | 600 nm | 0.552 | 777 ps | 0.218 | 1.54 ns | 0.231 | 157 ps | 820 ps | $4.8 \times 10^7$ $s^{-1}$ |
| | 650 nm | 0.678 | | 0.176 | | 0.146 | | | |
| | 700 nm | 0.738 | | 0.153 | | 0.110 | | | |
| THF | 600 nm | 0.767 | 481 ps | 0.087 | 1.47 ns | 0.146 | 216 ps | 478 ps | $4.0 \times 10^7$ $s^{-1}$ |
| | 650 nm | 0.700 | | 0.062 | | 0.242 | | | |
| | 700 nm | 0.659 | | 0.047 | | 0.294 | | | |

**Table 5.** Values of the calculated $R_0$ and rate constants for Förster type energy transfer, $k_{Förster}$, between the ICZ and BODIPY or DPP centered transitions and the experimental values of $\tau_1^{-1}$ as determined from the fluorescence decays and of $<k_{q,\,stat}>$ as determined from the stationary fluorescence experiments using Eq. 4 and 7.

| | | R (nm) | $R_0$ (nm) | $k_{Förster}$ ($s^{-1}$) | $<k_{q,stat}>$ ($s^{-1}$) | $\tau_1^{-1}$ ($s^{-1}$) |
|---|---|---|---|---|---|---|
| Toluene | Triad 1 | 1.26 | 4.79 | $4.83x10^{11}$ | $5.3x10^{10}$ | $4.2x10^{10}$ |
| | Polymer 1 | 1.26 | 4.81 | $4.95x10^{11}$ | $1.2x10^{10}$ | $1.4x10^{10}$ |
| | Polymer 2 | 1.46 | 3.55 | $3.29x10^{10}$ | $1.2x10^{9}$ | $3.70x10^{9}$ |
| Chloro-form | Triad 1 | 1.26 | 4.40 | $4.13x10^{11}$ | $1.7x10^{10}$ | $2.9x10^{10}$ |
| | Polymer 1 | 1.26 | 4.42 | $4.24x10^{11}$ | $1.3x10^{10}$ | $5.3x10^{10}$ |
| | Polymer 2 | 1.46 | 3.27 | $2.86x10^{10}$ | $1.1x10^{9}$ | $4.8x10^{9}$ |

# Improved spectral coverage and fluorescence quenching in donor-acceptor systems involving Indolo[3-2-b]carbazole and Boron-dipyrromethene (BODIPY) or Diketopyrrolo-pyrrole (DPP)

A. Khetubol,[1] S. Van Snick,[2] M.L. Clark[2], E. Fron,[1] E. Coutiño-González,[1] A. Cloet,[1] K. Kennes[1], Y. Firdaus[1], M. Vlasselaer,[2] V. Leen[2], W. Dehaen,[2] M. Van der Auweraer[1*]

[1]KULeuven, Chemistry Department, Molecular Imaging and Photonics, Celestijnenlaan 200F, B2404, 3001, Leuven, Belgium

[2]KULeuven, Chemistry Department, Molecular Design and Synthesis, Celestijnenlaan 200F, B2404, 3001, Leuven, Belgium

## Supportive Information

**Data S1: Fluorescence decays of the long wavelength emission of triad 1, polymer 1 and polymer 2 excited at 410 nm**

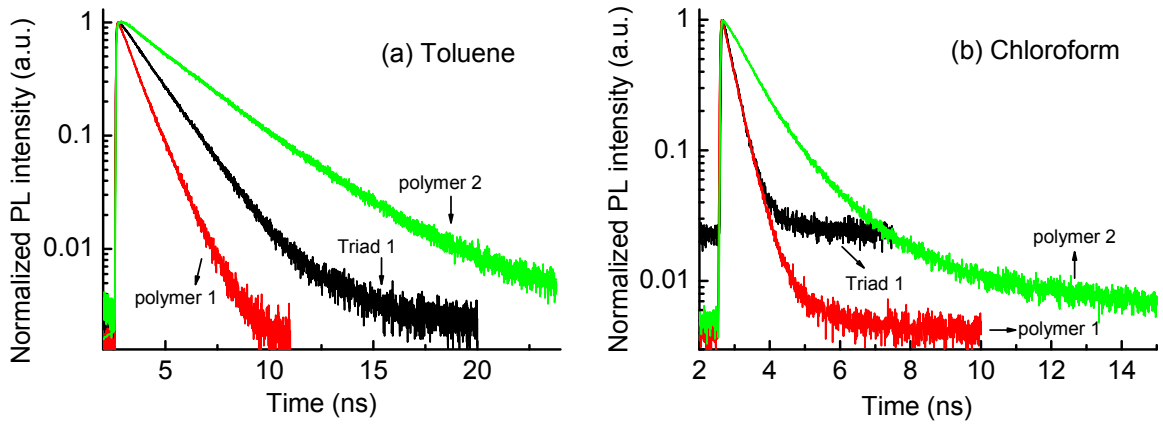


**Figure S1:** Normalized fluorescence decays of a solution of triad 1 (——), polymer 1 (——), and polymer 2 (——) in toluene (a) and chloroform (b), recorded the emission at the longer wavelength (See Table S1). The excitation occurred at 410 nm. The emission was recorded at 650 nm, 680 nm and 580 nm for respectively triad 1, polymer 1 and polymer 2 in toluene and at 730 nm, 700 nm and 680 nm for respectively triad 1, polymer 1 and polymer 2 in chloroform.

When the fluorescence decays were fitted to a sum of exponentials (Eq. S1) the fluorescence decay of triad 1, polymer 1 and polymer 2 in toluene and of polymer 1 in chloroform could be fitted to a sum of two exponentials while the fluorescence decay of triad 1 and polymer 2 in chloroform had to be fitted to a sum of three exponentials.

$$I(t) = \sum A_i \exp\left(-\,{}^{t}\!/\!_{\tau_i}\right) \qquad \text{(Eq. S1)}$$

The average fluorescence decay time, <τ> was calculated using equation S2.

$$\langle\tau\rangle = \frac{\sum A_i \tau_i}{\sum A_i} \qquad \text{(Eq. S2)}$$

**Table S1:** Amplitudes ($A_i$), fluorescence decay times ($\tau_i$) and average fluorescence decay time (<τ>) corresponding to the fluorescence decays shown in Figure S1. Excitation occurred at 410 nm.

| Samples | $\lambda_{em}$ (nm) | $A_1$ (%) | $A_2$ (%) | $A_3$ (%) | $\tau_1$ (ns) | $\tau_2$ (ns) | $\tau_3$ (ns) | ⟨τ⟩ (ns) |
|---|---|---|---|---|---|---|---|---|
| triad 1 (TL) | 650 | 7.6 | 92.4 | -- | 0.61 | 1.67 | -- | 1.59 |
| polymer 1 (TL) | 680 | 34.6 | 65.4 | -- | 0.49 | 1.02 | -- | 0.83 |
| polymer 2 (TL) | 580 | 4.1 | 95.9 | -- | 1.41 | 3.12 | -- | 3.05 |
| triad 1 (CF) | 730 | 18.5 | 80.5 | 1.1 | 0.05 | 0.29 | 1.39 | 0.26 |
| polymer 1 (CF) | 700 | 99.3 | 0.7 | -- | 0.35 | 1.80 | -- | 0.36 |
| polymer 2 (CF) | 680 | 61.7 | 36.1 | 2.2 | 0.59 | 1.21 | 4.32 | 0.90 |

**Data S2: Comparison of the excitation and absorption spectra of triad 1, polymer 1 and polymer 2**

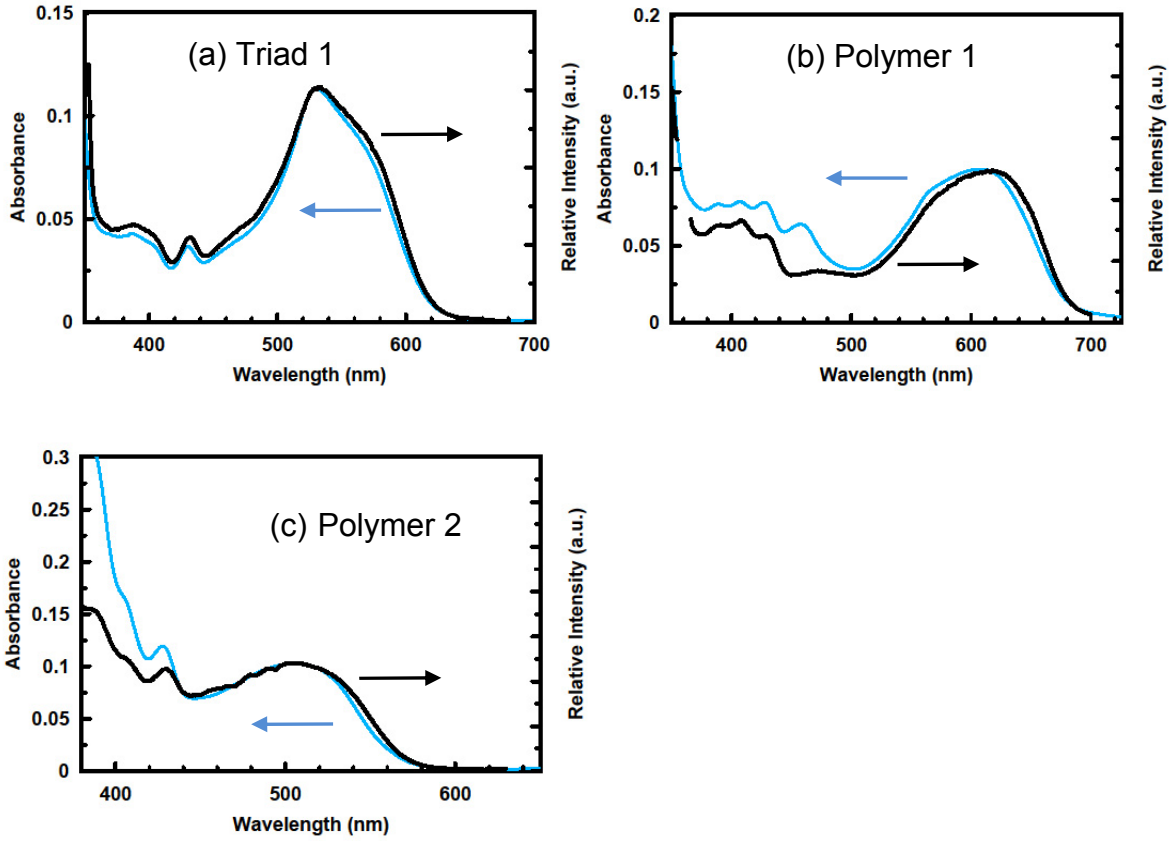


**Figure S2**: Absorption (————) and excitation (————) spectra of triad 1 (a), polymer 1 (b) and polymer 2 (c).in toluene. The excitation spectra were recorded for the emission at 700 nm, 720 nm and 650 nm for respectively triad 1, polymer 1 and polymer 2. The excitation spectra are normalized to the absorption spectra at the maximum of the long wavelength absorption band.

## Data S3: Transition dipole orientation in DPP 1

Mizuguchi *et al*. established that the transition dipole in diketopyrrolo pyrrole (DPP 1) to be oriented as pictured in Fig. S2.[1]

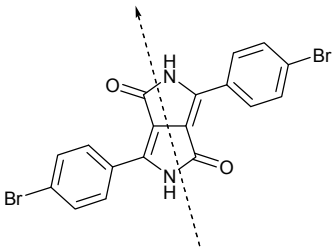


**Figure S3**: Transition dipole orientation in DPP 1

## Data S4: Excitation spectra of the films of triad 1 and polymer 1

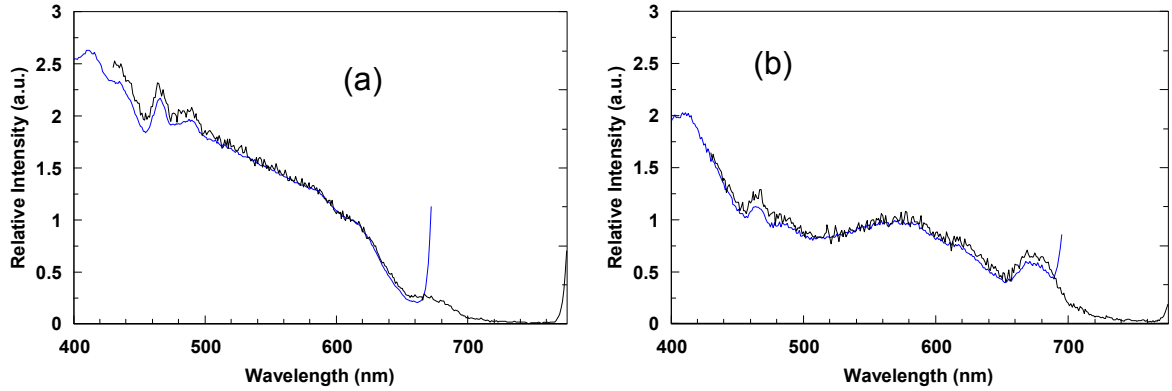


**Figure S4**: Excitation spectra of a film of (a) triad 1 and (b) polymer 1. The excitation spectra were recorded for an emission wavelength of 700 nm (_____) (720 nm for polymer 1) and 800 nm (_____). They are normalized to one at 612 nm (triad 1 and 575 nm (polymer 1)

## References


1. J. Mizuguchi, T. Imoda, H. Takahashi and H. Yamakami, Polymorph of 1,4-diketo-3,6-bis-(4′-dipyridyl)-pyrrolo-[3,4-*c*]pyrrole and their hydrogen bond network: A material for $H_2$ gas sensor, Dyes Pigm., 2006, **68**, 47-52.